Parallel evolution of phage resistance - virulence trade - offs during *in vitro* and nasal *Pseudomonas aeruginosa* phage treatment

Authors:

Meaghan Castledine[1], Daniel Padfield[1], Pawel Sierocinski[1], Jesica Soria Pascual[1], Adam Hughes[1], Lotta Mäkinen[1], Ville-Petri Friman[2], Jean-Paul Pirnay[3], Maya Merabishvili[3], Daniel De Vos[3], Angus Buckling[1]

Author affiliations:

[1]College of Life and Environmental Sciences, Environment and Sustainability Institute, University of Exeter, Penryn, Cornwall, TR10 9FE, U.K.
[2]Department of Biology, University of York, York, UK
[3]Laboratory for Molecular and Cellular Technology, Queen Astrid Military Hospital, Brussels, Belgium

Corresponding author: Meaghan Castledine (mcastledine96@gmail.com)

Author contributions: Patient isolates collected by JPP, MM and DDV. Study conceived and designed by MC, PS, JPP, DDV and AB. Experiments conducted by PS, JSP, AH, LM & MC. MC & DP analysed the data. All authors contributed significantly to the writing of the manuscript.

Data accessibility statement: All data and R code used in the analysis will be made available on GitHub and archived on Zenodo.

Acknowledgements: Genome sequencing was provided by MicrobesNG (http://www.microbesng.com)

Article type: Research article

Abstract

With rising antibiotic resistance, there has been increasing interest in treating pathogenic bacteria with bacteriophages (phage therapy). One limitation of phage therapy is the ease at which bacteria can evolve resistance. Negative effects of resistance may be mitigated when resistance results in reduced bacterial growth and virulence, or when phage coevolve to overcome resistance. Resistance evolution and its consequences are contingent on the bacteria-phage combination and their environmental context, making therapeutic outcomes hard to predict. One solution might be to conduct "*in vitro* evolutionary simulations" using bacteria-phage combinations from the therapeutic context. Overall, our aim was to investigate parallels between *in vitro* experiments and *in vivo* dynamics in a human participant. Evolutionary dynamics were similar, with high levels of resistance evolving quickly with limited evidence of phage evolution. Resistant bacteria – evolved *in vitro* and *in vivo* - had lower virulence. *In vivo*, this was linked to lower growth rates of resistant isolates, whereas *in vitro* phage resistant isolates evolved greater biofilm production. Population sequencing suggests resistance resulted from selection on *de novo* mutations rather than sorting of existing variants. These results highlight the speed at which phage resistance can evolve *in vivo*, and *in vitro* experiments may give useful insights for clinical evolutionary outcomes.

46 **Introduction**

47 By 2050, as many as 10 million people may die annually from antimicrobial resistant infections
48 (WHO, 2019). To combat this threat, phage therapy is being increasingly researched as a
49 complement to antibiotics (Abedon, 2019; Kwiatek et al., 2020). Phage therapy uses viruses
50 (phage) that infect pathogenic bacteria to clear infections (Kwiatek et al., 2020). Phage therapy
51 has several advantages to antibiotics by being species specific (thus not harming beneficial
52 microbiota) (Koskella and Meaden, 2013) and self-amplifying at infection sites (Górski et al.,
53 2015). A major consideration with the use of therapeutic phages is the ease and speed (sometimes
54 within hours) at which bacteria can evolve resistance, which can greatly limit the therapeutic
55 potential of phages (Jariah and Hakim, 2019; Torres-Barceló, 2018; Torres-Barceló and Hochberg,
56 2016). However, phages may contribute to reducing the severity of infections even after resistance
57 evolves. First, phage can sometimes evolve to overcome this resistance (i.e. bacteria-phage
58 coevolution) and so they may continue lowering bacterial densities (Gandon et al., 2008; Hampton
59 et al., 2020). Second, resistance can trade-off against bacterial growth rates and virulence; as the
60 alteration or loss of bacterial surface structures, typically associated with phage resistance, can
61 affect other fitness-related phenotypes such as nutrient uptake, biofilm formation and binding of
62 host receptors (Mangalea and Duerkop, 2020). Predicting the evolutionary outcome of phage
63 therapy is therefore of crucial importance (Abedon, 2017).

64 Bacteria-phage dynamics and its consequences for phage therapy are highly context-
65 specific (Gandon et al., 2008; Hampton et al., 2020). Both human clinical and animal models
66 studies report a range of outcomes with differing phage therapy success, and differences in the
67 extent of resistance evolution and associated costs and virulence (Abedon, 2019; Brix et al., 2020;
68 Kwiatek et al., 2020; Leitner et al., 2021). One solution to better understand the outcome of *in vivo*

69 therapy is to conduct controlled *in vitro* experiments with the relevant organisms. However, while
70 most of our understanding of the ecology and evolution of bacteria-phage interactions comes from
71 highly controlled *in vitro* environments (Gandon et al., 2008; Hampton et al., 2020), we do not
72 know how well *in vitro* dynamics mirror *in vivo* dynamics quantitatively or even qualitatively.

73 There are good reasons to expect the outcomes may be very different. *In vivo* environments
74 are expected to be more stressful for bacteria owing to limiting resources, presence of immune
75 cells and competing microbiota (Everest, 2007). Consequently, these conditions may differ
76 significantly from studies of bacteria-phage coevolution in nutrient rich microcosms which could
77 drive differences in (co)evolutionary dynamics and associated trade-offs (Gandon et al., 2008;
78 Hampton et al., 2020). In order to evolve phage resistance, bacteria must have sufficient mutation
79 rates supplied either by high resources (facilitating rapid growth) or population mixing (genetic
80 exchange) (Gandon et al., 2008; Hampton et al., 2020; Morgan et al., 2010, 2005; Pal et al., 2007).
81 Smaller population sizes *in vivo* may therefore limit resistance. Moreover, resistance costs and
82 trade-offs may be greater as a consequence of the additional selection pressures facing bacteria,
83 which may limit selection for resistance, making it easier for phage to overcome resistance, or
84 reduce growth rates and virulence (Buckling et al., 2006; Scanlan et al., 2015).

85 Consequently, the main aim of this research was to determine how well *in vitro* bacteria –
86 phage coevolutionary dynamics mirror dynamics in a clinical context. As a starting point, we
87 followed bacteria - phage coevolutionary dynamics during a phage-mediated decolonisation trial
88 in parallel with the dynamics between the same bacteria and phage *in vitro*. The nasal cavity can
89 act as a source of infection, notably from highly drug-resistant *Pseudomonas aeruginosa* and
90 *Staphylococcus aureus* when patients undergo hospitalisation and are treated with broad spectrum
91 antibiotics (Mainz et al., 2009; Wertheim et al., 2004). The trial was conducted to try and

92 decolonise intensive care (ICU) patients with *P. aeruginosa* and *S. aureus*, using a phage cocktail
93 prior to antibiotic treatment in prevention of ICU infections with these pathogens. Mucirocin (trade
94 name Bactroban) and chlorhexidine are routinely used for nasal decolonisation in such contexts,
95 but extensive use of these agents has led to resistance and new nasal antiseptics need to be
96 considered (Edgeworth, 2011). We focused on a single patient, in which we could detect *P.*
97 *aeruginosa* at the beginning of the trial and both *P. aeruginosa* and phage during treatment.
98 Decolonisation of *P. aeruginosa* was ultimately successful in this patient. We used the pre-
99 treatment *P. aeruginosa* isolates and evolved these populations *in vitro* in the absence and presence
100 of treatment phages. We measured bacteria-phage (co)evolution and while we found extensive
101 resistance evolution both *in vivo* and *in vitro*, we only found evidence of limited phage infectivity
102 evolution *in vitro*. We determined the consequences of resistance, with respect to virulence, and
103 the possible mechanisms linking this resistance – virulence trade – off using phenotypic (growth
104 rate, biofilm assays) and metagenomic analyses for the *in vivo* and *in vitro* populations. As we
105 only had access to samples from a single patient, we did not have a control group to understand
106 the impact of phage application frequency *in vivo*. However, we were able to do this in our *in vitro*
107 experiments, where we included two phage treatments: one where phages were added repeatedly
108 (mimicking multiple phage doses during *in vivo* phage treatment) and one where phage were added
109 once (at the start of the experiment). By comparing these treatments and to the *in vivo* treatment,
110 we were able to gain further insight into how multiple phage doses may affect phage therapy.
111

112 **Methods**

113 **Ethics statement**

114 The decolonisation study protocol was approved by the Leading Ethics Committee of the
115 "Université Catholique de Louvain" (Avis N°: B-403201111110). The study was performed in
116 accordance with the ethical standards as laid down in the Declaration of Helsinki and as revised in
117 2013. The patients gave informed consent and their anonymity was preserved.

118 **Patient information, bacteria and phage strains and phage-bacteria evolution *in vivo***

119 Bacterial isolates were sampled from a patient as part of a clinical trial in Brussels, Belgium. The
120 patient (85 years old, male) had been admitted to an intensive care unit in 2015 for treatment of
121 burns (10% body area). Independent of his burns, a nasal colonisation of *P. aeruginosa* was
122 observed. Here, the patient was treated every day with a three-phage cocktail (BFC-1) for five
123 days, which consisted of two phages (14-1 and PNM) that could lytically infect *P. aeruginosa*.
124 The phage cocktail included a third phage that specifically infects *S. aureus* bacterium but was not
125 detected in this patient. This phage cocktail has been characterised to ensure no prophage elements
126 are present or that the phage carry toxin-encoding genes that may increase bacterial resistance
127 and/or virulence (Merabishvili et al., 2009). Furthermore, a purification process including the
128 removal of endotoxins in phage production was used to ensure such waste products cannot harm
129 patients (Merabishvili et al., 2009). As 14-1 infects via a lipopolysaccharide (LPS) (Betts et al.,
130 2014; Kropinski et al., 1977) receptor and PNM uses type IV pili (Ceyssens et al., 2011), resistance
131 to one phage is unlikely to result in cross-resistance and neither phage should compete for receptor
132 sites. Swabs of both nasal cavities were taken on day 0 (commencement of phage therapy), 2, 4, 7
133 and 13 and frozen at -80 °C in lysogeny broth containing 20% glycerol. Individual *P. aeruginosa*
134 isolates were obtained by plating swabs onto cetrimide selection plates. Colonies were picked and
135 inoculated into Luria broth (LB) and grown overnight, shaking at 180 r.p.m., at 37 °C to achieve
136 high cell densities. Additionally, swabs were soaked in LB broth to amplify phage overnight in the

137 same conditions. Phage was isolated from overnight cultures via chloroform extraction: 100 µL of
138 chloroform was added 900 µL of culture, vortexed and then centrifuged (14000 r.p.m., 1 min); the
139 supernatant was isolated and stored at 4 °C. Culture samples were frozen in 80% glycerol (final
140 concentration 40%) at -80 °C. Spot assays on lawns of *P. aeruginosa* P573 (a phage susceptible
141 control strain) confirmed the presence of phage at all time-points. Twelve individual plaques were
142 picked at each time-point and amplified with an overnight culture of P573 to obtain clonal isolates.
143 Individual isolates of *P. aeruginosa* were isolated from days 0 (n = 24), 2 (n = 8) and 4 (n = 2) for
144 use in this study and swabs were negative on days 7 and 13. Individual isolates were treated as
145 biological replicates for *in vivo* study.

146 **Experimental *in vitro* phage-bacteria evolution**

147 To examine whether findings *in vitro* are consistent with *in vivo* bacteria-phage (co)evolution,
148 phage therapy was replicated in the laboratory. We used two treatments: (1) phage added "once",
149 at the start of the experiment, and (2) phage added at every second transfer ("repeated" treatment).
150 The repeated phage treatment aimed to emulate the conditions of the clinical trial while the "once"
151 condition was used to assessed whether repeated doses change the observed dynamics. The phages
152 were identical to the two lytic phages (14-1 and PNM) used in the clinical trial. A control group in
153 which bacteria evolved in the absence of phage was set up and there were 6 biological replicates
154 in the control and each phage treatment.

155 Prior to experimental set-up, *in vivo* ancestral isolates (n = 24, same isolates as day 0) were
156 individually amplified in LB media and cultured at room temperature for two days. Cell densities
157 were estimated via optical density (wavelength 600 nm; OD_{600}) measures. Cultures were
158 centrifuged (14000 r.p.m., 3 min), the supernatant removed, and resuspended in M9 buffer to
159 equalise cell densities. These were added to a master-mix in which isolates were equally

160 represented in equal ratio (total 10^8 CFUs / mL; ~4 x 10^6 CFUs / mL of each isolate). 100 µL of
161 master-mix (10^7 CFUs; ~4 x 10^5 CFUs per isolate) was inoculated into 5 mL LB media. 100 µL of
162 phage was added to treatment microcosms at a total multiplicity of infection (MOI) of 0.5.
163 Microcosms were cultured, shaken (180 r.p.m.), at 37 °C. 1% transfers (50 µL culture into 5 mL
164 LB) took place every two days for a total of 12 days. At each transfer, culture samples were frozen
165 in glycerol, and in the phage treatments, phage were extracted as described previously. Cultures
166 were diluted and plated from frozen stocks onto LB agar and incubated for two days at 37 °C.
167 From each biological treatment replicate and time-point (days 4, 8 and 12), 16 bacterial colonies
168 were picked (96 total colonies) for time-shift assays to measure coevolutionary changes. An
169 additional 24 isolates were isolated at day 12 from each treatment and control group replicate for
170 bacterial virulence assays. Individual isolates are treated throughout as biological replicates nested
171 within their treatment (biological) replicate. Picked isolates were individually amplified in LB
172 media overnight before being frozen as described previously.

173 **Measuring resistance-infectivity (co)evolution**

174 To assess whether bacteria and phage had coevolved *in vivo* and *in vitro*, resistance assays were
175 conducted where bacteria were exposed to phage populations from the same/contemporary, past,
176 and future time-points (time-shift assays) (Buckling and Rainey, 2002). If bacteria and phage
177 coevolved, both bacteria and phage would show significant changes in resistance and infectivity,
178 respectively, through time. Increases in resistance and infectivity would be indicative of arms race
179 dynamics (ARD), while non-directional changes would be indicative of fluctuating selection
180 dynamics (FSD) (Lopez Pascua et al., 2014). Infectivity/resistance was determined by spot assays
181 in which 100 µL of overnight bacterial cultures was added to 5-8 µL soft LB agar overlay and 5
182 µL of each ancestral phage, or evolved phage mixture, was spotted onto the overlay. For *in vivo*

183 isolates, ancestral isolates (isolated pre-phage therapy) and bacterial isolates from days 2 and 4
184 were tested against the phage clonal isolates from days 2, 4 and 7. A bacterial isolate was scored
185 as susceptible (1 = susceptible, 0 = resistant) if at least one of twelve clonal phage isolates could
186 infect. *In vitro* isolates from days 4, 8 and 12 were tested (16 colonies per time-point) against phage
187 populations isolated from each time-point. In addition, we assessed the infectivity of both ancestral
188 phage against the ancestral bacteria (n = 24), the *in vivo* isolates (n = 8), and the *in vitro* populations
189 from day 12 (n = 24 per treatment replicate).

190 **Virulence assays**

191 Changes in bacterial virulence were measured using a *Galleria mellonella* infection model (Tsai
192 et al., 2016). Virulence of all ancestral (n = 24) and *in vivo* isolates (n = 10) were measured,
193 however two *in vivo* isolates (from day 2 of phage therapy) were excluded from analyses as time
194 of death was not accurately determined. As few isolates remained phage susceptible (n = 3), these
195 were pooled with phage resistant isolates to determine a change in virulence from pre- (ancestral,
196 n = 24) to post-phage treatment (n = 8). For *in vitro* isolates, where possible, one resistant and one
197 susceptible (to ancestral phage) isolate were selected from each treatment replicate to give a total
198 of 12 resistant and 12 susceptible isolates, with 14 isolates from the "phage added once" and 10
199 isolates from the "phage added repeatedly". As some treatment replicates contained no susceptible
200 isolates, multiple resistant isolates were chosen (Table S1). Seven *in vitro* isolates evolved
201 resistance to one phage only (single resistance), therefore their virulence was measured to assess
202 whether changes in virulence were mediated by resistance to one or both phages. The virulence of
203 *in vitro* isolates was contrasted to six isolates from the control group isolated from 6 independent
204 replicates.

205 For each bacterial isolate (total of 56 biological replicates), 20 *G. mellonella* larvae (20
206 technical replicates) were infected with 10 µL (~100 CFUs) of overnight culture (cells resuspended
207 in M9 buffer) using a sterile syringe. Twenty *G. mellonella* larvae were injected with 10 µL of M9
208 buffer as a technical control. Survival of each larvae was assessed every two hours for up to 58
209 hours.

210 **Growth rate assays**

211 We measured bacterial growth rates as a potential mechanism underlying virulence variation and
212 cost of resistance for ancestral and all evolved isolates (*in vitro* and *in vivo*) tested in the virulence
213 assay. Growth curves were measured in a 96 well plate with 10 µL of culture (1.0 x 10^5 CFUs)
214 from each isolate inoculated into individual wells containing 140 µL LB broth. 26 wells remained
215 as blank controls. The plate was incubated in an OD reader (Biotek Instruments Ltd) at 37 °C in
216 shaken conditions and OD_{600} was measured every 20 mins for 24 hours to estimate changes in
217 cellular density. Growth curves were independently replicated 3 times (technical replicates).

218 **Biofilm assay**

219 Biofilm production of isolates isolated for virulence and growth rate assays was measured using a
220 resazurin assay, based upon a previously described protocol (Peeters et al., 2008). Overnight
221 monocultures were diluted to 0.1 OD_{600} (~10^9 CFU/mL) into M9 buffer. 100 µL of each culture
222 was inoculated into a sterile 96 well plate and incubated at 37 °C for 4 hrs for cellular adhesion.
223 Then, the supernatant was removed, and wells were washed gently with 100 µL of M9 buffer by
224 pipetting up and down 3 times. 100 µL of fresh LB media was added to each well including 25
225 controls (no bacteria) and plates were incubated for 16 hrs. Liquid was removed and wells were
226 washed with 100 µL M9 buffer. 100 µL of fresh M9 was added followed by 10 µL resazurin
227 solution (final resazurin concentration: 100 µM). Fluorescence (λex: 560 nm and λem: 590 nm)

228 was measured after 1 hr incubation. Biofilm assays were independently replicated 3 times
229 (technical replicates).

230 **Sequencing**

231 We sequenced the genomes of the bacterial isolates used for the *in vitro* experiment to establish to
232 what extent evolution was driven by *de novo* mutation or selection on existing genetic variation.
233 This is especially pertinent as the experiment did not start from a clonal population, rather from
234 24 isolates (which included an isolate that was resistant to one phage). At the end of the
235 experiment, we picked 24 isolates, extracted DNA from isolates individually and performed whole
236 genome sequencing (WGS) on pools of the bacterial isolates that were isolated from each replicate
237 (pool-seq). Total DNA extraction (19 pooled-isolate samples) was performed using the "Qiagen
238 QIAmp DNA Mini Kit" following the manufacturer's instructions. An Illumina HiSeq 2000
239 sequencer was used to generate 100 bp paired reads from a 500 bp insert library.

240 Reads were trimmed for the presence of Illumina adapter sequences and for quality scores
241 below 10 using *TrimGalore* (v0.6.4_dev, powered by *Cutadapt*). *TrimGalore* also removed any
242 paired end reads when one of the paired end reads was shorter than 20 bp. Trimmed reads were
243 mapped to the *P. aeruginosa* UCBPP-14 reference genome (Locus: NC_008463) with *bwa-mem*
244 (v0.7.17-r1188), and duplicates were marked using *samblaster* (v0.1.24). Subsequent bam files
245 were split into mapped and unmapped reads, sorted and indexed using *samtools* (v0.1.19-
246 44428cd). Across all files, ~93% of the reads mapped to the reference genome (minimum 92.5%),
247 giving on average ~12,000,000 reads per replicate (minimum 8,807,569). Variants were called
248 identified using *freebayes* (v1.3.2-dirty) with ploidy set to 24 (*-p 24*) and we assumed pooled
249 samples with a known number of genome copies (*--pooled-discrete*). Due to the high ploidy of the

250 pooled samples, we reduced the number of alleles that are considered at the cost of sensitivity to
251 lower frequency alleles at multiallelic loci by setting *--use-best-n-alleles 4*.
252 Next, we compiled the vcf files (standard output of SNP callers) into *R* using the package
253 *vcfR* and kept only the variants which were sequenced at a depth within two standard deviations
254 of the mean. Variants were further filtered to retain only those with quality scores >30. We used
255 the two replicate sequencing runs of the same samples to conservatively identify variants; variants
256 were only kept if they occurred in both sequencing runs and if there was less than 0.3 difference
257 in frequency between runs. We then only kept variants that had different frequency than the
258 ancestor (> 1/24 difference in frequency). To identify significant differences in genetic variants
259 (SNPs and indels) between treatments, we first filtered unique that were present in at least three
260 replicates of any treatment. This identified 960 potential variants. We then performed a Wilcoxon
261 test on each variant, with frequency as the response variable and treatment (control, phage added
262 once, and phage added repeatedly) as the predictor. Significant genetic variants were identified if
263 the adjusted p value (*fdr* method) was < 0.05. Of these significant changes, 160 were existing
264 genetic variants and 120 were novel mutations. We then checked where each variant was in the
265 genome and only retained variants that were occurred in a gene. After these steps, 50 genetic
266 variants were identified in genes of known function, and 236 in genes of unknown function.
267 For the *in vivo* isolates, DNA extraction and whole genome sequencing on each isolate
268 individually by MicrobesNG using in-house protocols ("MicrobesNG Sequencing Service
269 Methods v20210419," n.d.). Whole genome sequencing was carried out on each isolate
270 individually by MicrobesNG using Illumina sequencers (HiSeq/NovaSeq) to create 250 bp paired
271 end reads. In-house processing by MicobesNG trimmed the adapters and removed reads with a
272 quality < 15. We then processed the reads as for the pooled sequencing, except ploidy was set to

273 1 when using *freebayes*. On average, 81% of reads mapped back to the reference genome, but there
274 was more variation as compared to the *in vitro* experiment, with a minimum of 44% and a
275 maximum of 94%. As we only had isolates from a single patient, there was limited statistical
276 analysis we could do, so we primarily concentrated on whether the significant changes found *in*
277 *vitro* were also present in the *in vivo* isolates.

278 **Statistical analyses**

279 All data was analysed using R (v. 4.0.3) in RStudio (Team, 2013) and all plots were made using
280 the package "*ggplot2*" (Wickham, 2016). Model simplification was conducted using likelihood
281 ratio tests and Tukey's post-hoc multiple comparison tests were used to identify the most
282 parsimonious model using the R package "*emmeans*" (Lenth, 2018). First, we established whether
283 bacteria and phage had coevolved *in vivo* and in each *in vitro* treatment using general linear mixed
284 effects models. Models were fitted using the package "*lme4*" (Bates et al., 2014). *In vivo* isolates
285 from day 4 were excluded as their small sample size (n = 2) prevented model convergence. For *in*
286 *vivo* isolates: infection (1 = susceptible, 0 = resistant) was analysed against phage time-point (fixed
287 effect) with a binomial error structure. A random effect of "isolate" was included to account for
288 the same bacterial isolate being used in infectivity assays across each phage time-point. For *in*
289 *vitro* analyses, the proportion of isolates infected was analysed against fixed effects of phage and
290 bacterial time-points with separate models for each phage treatment. To see if there were any
291 differences in phage resistance to ancestral phage or *in vitro* phage isolates at the end of the
292 experiment, the proportion of isolates infected was analysed against fixed effects of phage
293 treatment and phage type (ancestral or end – point phage). All *in vitro* models included a random
294 effect of "replicate" (which treatment replicate isolates had been isolated from) with a binomial
295 error structure.

296 Virulence of bacterial isolates was analysed using survival curves from the survival of
297 *Galleria* infected with different isolated isolates. Survival curves were fitted using Bayesian
298 regression models using the package "*rstanarm*" (Goodrich, 2020) and parameters were estimated
299 using "*tidybayes*" (Kay and Mastny, 2020). For all models, we fit a proportional hazards model
300 with an M-splines baseline hazard. Models were ran for 3000 iterations and 3 chains were used
301 with uninformative priors. Model convergence was assessed using Rhat values (all values were 1)
302 and manually checking chain mixing. For all models, log hazards were estimated for each
303 treatment value and hazard ratios were calculated as the exponential of the difference between two
304 log hazards. A hazard ratio below one indicates a decrease in virulence compared to the baseline
305 treatment, with a value above one indicating an increase in virulence. Median hazard ratios with
306 95% credible intervals that do not cross 1 indicate a significant difference in virulence between
307 two factors. Proportion of *Galleria* that died and mean time to death of *Galleria* that died were
308 calculated as summary statistics for each treatment.

309 For virulence analyses of *in vivo* isolates, treatment (pre- or post-phage therapy) was the
310 only predictor of survival, with a random effect of "isolate" added to account for multiple *G.*
311 *mellonella* larvae being infected by the same isolate. For the *in vitro* isolates, survival was analysed
312 against interacting fixed effects of resistance (resistant, single resistant, susceptible) and treatment
313 (no phage added, phage added once, phage added repeatedly). Here, an additional random effect
314 of "replicate" was included to account for clonal non-independence.

315 Biofilm productivity of *in vitro* isolates was estimated using linear mixed effects models.
316 Biofilm production (fluorescence 560/590nm) was log transformed to account for the data being
317 abundance-based. Biofilm production was averaged over each technical replicate for each
318 biological replicate (individual bacterial isolates). Biofilm production was used as the response

319 variable, and explained with interacting fixed effects of treatment and phage resistance, while
320 treatment replicate was included as a random effect. One outlier was removed each from the
321 susceptible and control groups as these were likely contamination (full data cleaning process and
322 impact on parameter estimates explained in the SI and effects of outlier removal on estimates
323 shown in Tables S3 & S4). Due to the low number of isolates, biofilm productivity of *in vivo*
324 isolates from before and after phage treatment as well as phage susceptible and resistant isolates
325 were estimated using a non-parametric bootstrap using the R package "*boot*" (Canty and Ripley,
326 2021). Non-overlapping 95% CIs were interpreted as being significantly different.

327 Before growth rate analyses, data points from the first 2.5 hrs were removed as a sharp
328 increase in OD was observed before lag phase independent of exponential growth (Figure S1).
329 Growth rates were estimated using a rolling regression taking the steepest slope of the linear
330 regression between *ln* OD_{600} and time in hours in a shifting window of every 7 time points (every
331 2.3 hrs). Growth rate was averaged over each technical replicate for each biological replicate
332 (individual bacterial isolates). For *in vitro* isolates, growth rate was analysed against treatment and
333 resistance in a linear mixed effects model with a random effect of treatment "replicate". Growth
334 rates of isolates pre- and post-phage treatment, and resistant and susceptible *in vivo* isolates were
335 compared using 95% confidence intervals (CIs) that were estimated using a non-parametric
336 bootstrap.

337 To look at genetic differences *in vitro*, we calculated several commonly used metrics using
338 the frequency data of the 50 variants in known genes that differed significantly between our
339 treatments: (1) the genetic distance from the ancestral population, calculated as the sum of the
340 difference of the proportion of each SNP/indel in each population from the ancestral proportion;
341 (2) the number of unique *de novo* SNPs/indels in each population; (3) alpha diversity, calculated

342 using a modified version of the Hardy-Weinberg equilibrium, such that $\alpha = \sum(1 - p_i^2 - q_i^2)$,
343 where i is the position of each SNP/indel, p is the proportion of the SNP/indel and q is $1 - p$. This
344 is equivalent to expected heterozygosity. Differences between these metrics were analysed using
345 linear models. To test whether consistent genetic differences occur within treatments, we
346 performed non-metric multidimensional scaling on the Euclidean distance matrix of SNPs/indels
347 and their proportions in each population using "*metaMDS*" in the R package "*vegan*". Nonmetric
348 multidimensional scaling aims to collapse information from multiple dimensions (*i.e.*, from
349 different populations and multiple SNPs/indels per population) into just a few, allowing
350 differences between samples to be visualized and interpreted. Permutational ANOVA tests were
351 run using "*vegan::adonis*", with Euclidean distance as the response term and treatment as the
352 predictor variable with 9999 iterations. Changes in beta-diversity were examined using
353 "*vegan::betadisper*" using the same response and predictor variables as in the PERMANOVA.
354 For the *in vivo* sequencing, we looked for the presence of variants found to be significant
355 *in vitro* in the *in vivo* isolates. To see if any of the genetic changes could explain differences in
356 phenotypes of the isolates, we did non-metric multidimensional scaling as described previously.
357 Phenotypic traits of the isolates (virulence, growth rate, resistance profile, and biofilm production)
358 were then mapped onto the resulting NMDS plot to see whether observed genetic changes
359 correlated with any changes in phenotype (Figure S2).
360

361 **Results**

362 **Resistance and infectivity (co)evolution**

363 *In vivo*

364 Resistance to phage can evolve via *de novo* mutations or selection on pre-existing resistance and
365 we therefore tested the resistance of ancestral bacterial isolates to ancestral phage and pooled phage
366 isolates isolated *in vivo*. Of the 24 ancestral isolates isolated *in vivo* at day 0, 23 were susceptible
367 to both the ancestral phage (14-1 and PNM) while one was resistant to 14-1 but susceptible to
368 PNM. In subsequent tests of phage resistance to phage isolates isolated *in vivo*, all ancestral
369 bacteria were susceptible to phage (Figure 1a). We considered whether bacteria and phage
370 coevolved *in vivo* using time-shift assays to determine changes in resistance and infectivity through
371 time. After two days, we saw evidence of resistance evolution, with more than half of bacterial
372 isolates being resistant to ancestral phage. 1 of 2 isolates isolated at day 4 were phage resistant and
373 no *P. aeruginosa* was detected from nasal swabs after this time point. Although both bacterial
374 populations from days 2 and 7 showed observationally higher phage resistance (87.5% day 2,
375 100% day 4) against day 2 phage, this was non-significantly different to resistance shown to
376 ancestral phage and phage from days 4 and 7 (Tukey HSD: $p > 0.05$; Table S2; Figure 1a). This
377 non-significance is likely due to low statistical power from limited clonal numbers (only 8 isolates
378 from day 2) and the consistency of resistance levels in bacterial populations from day 2 apart from
379 to its contemporary phage; overall, results showed equal levels of phage resistance over time *in*
380 *vivo*. The absence of changes in phage infectivity through time did not warrant further investigation
381 of the population dynamics of the two inoculated phages.
382

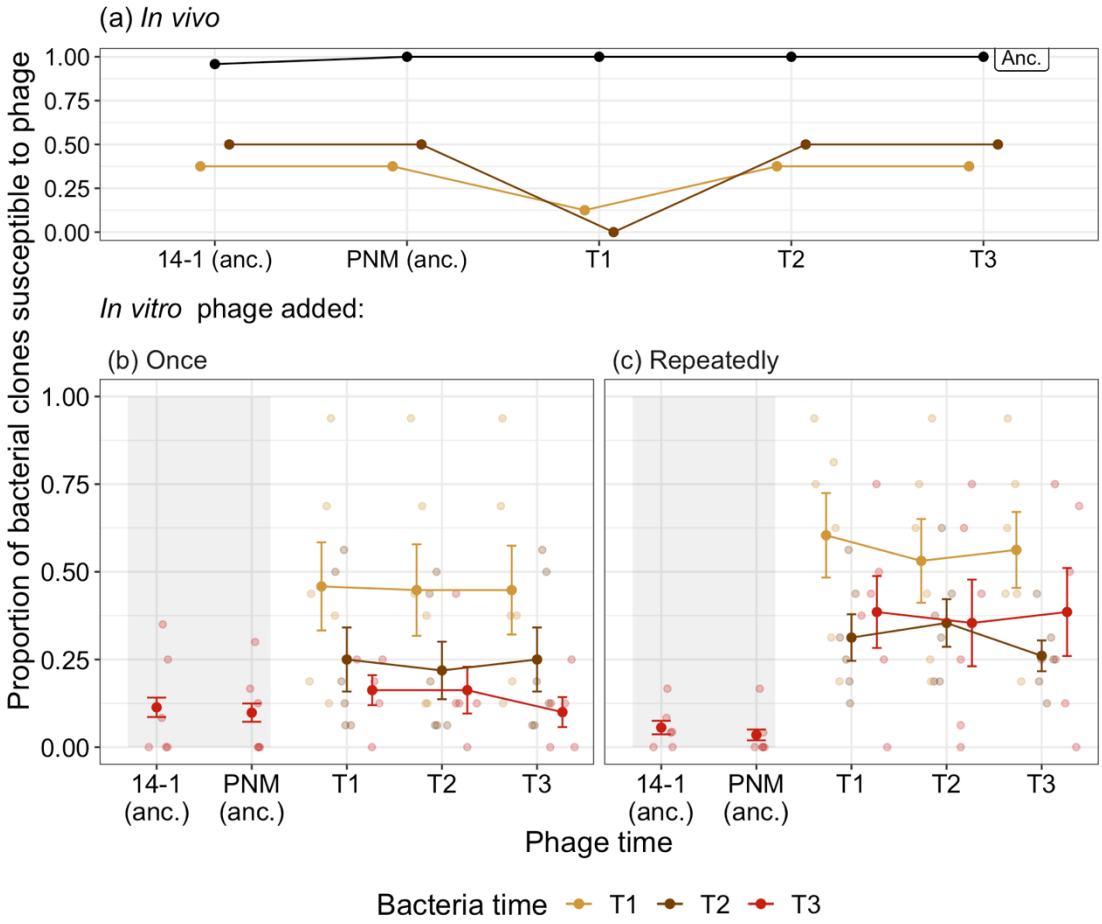

Figure 1. Time-shift assays of bacterial evolution and phage during phage therapy. The proportion of phage susceptible bacterial isolates from (a) ancestral (pre-phage therapy, "Anc."), and days 2 (T1) and 4 (T2) of *in vivo* (clinical) phage therapy (n = 8) tested against ancestral phage ("anc.": 14-1 and PNM) and phage isolates from days 2 (T1), 4 (T2) and 7 (T3). The same ancestral bacterial isolates are evolved *in vitro* with phage added either (b) once, at the start of the experiment for comparison to (c) in which phage are added repeatedly, emulating clinical treatment. For (b) and (c) the proportion of bacterial isolates susceptible to phage at three time-points (T1 - T3: days 4, 8 and 12 of coevolution) is presented with small points as independent treatment replicates. Resistance of bacteria isolated at T3 to ancestral phage ("Anc.": 14-1 and PNM) is indicated within the shaded region, note that these isolates are distinct from those tested against phage from T1-T3. Filled points are the mean proportion of resistant isolates across replicates. Bars = ±SE.

394

395 *In vitro*

396 We used the same bacterial isolates and phages to determine how well the *in vivo* evolutionary
397 dynamics paralleled *in vitro* experiments in the lab. To assess the impact of phage application
398 schedule, we added phages once at the start of the experiment, repeatedly (as was the case *in vivo*)
399 or not at all. The dynamics in the phage treatments largely mirrored the *in vivo* dynamics.
400 Resistance to phage increased through time, reaching comparable levels to that observed *in vivo*
401 (>50%). While phage resistance increased in both phage treatments (ANOVA comparing models
402 with and without bacterial time: phage added: once $\chi^2_2 = 79.08$, $p < 0.001$; repeatedly $\chi^2_2 = 45.30$,
403 $p < 0.001$; Figure 1b, c), there was a significantly higher proportion of phage resistant bacteria in
404 the treatment where phages were added once (90.81%, ±SE = 0.0003) compared to when phages
405 were added repeatedly (66.7%, ±SE = 7.64; Tukey HSD comparing phage added once and
406 repeatedly treatments: estimate = -1.63, z-ratio = -3.75, p = 0.0002; Figure 1b, c). All isolates from
407 the control condition were susceptible to ancestral phages.

408 The lower resistance of bacteria when phages were added repeatedly was driven by
409 evolution of increased phage infectivity. When phages were added once, resistance to ancestral
410 phage (14-1: 88.64%, ±SE = 2.77; PNM: 90.15%, ±SE = 2.60) did not differ relative to phage
411 isolated at the end of experimental evolution (90.0%, ±SE = 4.27; Tukey HSD comparing end-
412 point phage resistance to contemporary phage to resistance to 14-1 (p = 1.0) and PNM (p = 0.938;
413 Figure 1b). However, when phages were added repeatedly, resistance to ancestral phage (14-1:
414 94.41%, ±SE = 1.93; PNM: 96.5%, ±SE = 1.54) was significantly higher than to phage isolated at
415 the end of experiment (61.5%, ±SE = 12.5), indicative of increased phage infectivity (Tukey HSD
416 comparing end-point phage resistance to contemporary phage to resistance to 14-1 ($p < 0.001$) and

417 PNM ($p < 0.001$); Figure 1c). We saw no further evidence of phage evolution in either treatments,
418 with phage resistance being independent to the time point from which phage were isolated during
419 experimental evolution (ANOVA comparing models with and without phage time: phage added:
420 once $\chi_2^2 = 0.41$; $p = 0.814$; repeatedly $\chi_2^2 = 0.68$; $p = 0.713$; Figure 1c). This suggests the increase
421 in phage infectivity evolved before the first sampling time point (the second transfer, or 96 hours).
422 The absence of any further changes in phages during experimental evolution did not warrant
423 further investigation of the population dynamics of the two inoculated phages.
424
425 **Phage resistance-virulence trade-offs**
426 We next assessed whether phage application altered the virulence of *P. aeruginosa* populations *in*
427 *vivo* and *in vitro* using a *G. mellonella* infection model. Here, virulence can be calculated as the
428 inverse of *G. mellonella* survival over time: the more virulent the bacterial isolate, the shorter the
429 time until death. *In vivo*, phage therapy reduced bacterial virulence by 95.5% on average (median
430 hazard ratio = 0.045, 95%CI = 0.012 – 0.163). When inoculated with bacteria isolated before phage
431 therapy, 479 (99.7%) of *G. mellonella* died within 46 hours, with death occurring at a mean time
432 of 15 hours (Figure 2a). In contrast, after phage therapy, bacteria killed only 70% of *G. mellonella*
433 within 50 hours, with mean time of death occurring at 20.5 hours (Figure 2a).
434 We also saw a reduction in virulence *in vitro* when populations had evolved with phage
435 compared to without phage. Bacteria in the phage added once and phage added repeatedly
436 treatments were 96.15% (median hazard ratio = 0.0385, 95%CI = 0.011 – 0.124) and 89.8%
437 (median hazard ratio = 0.102, 95%CI = 0.0294 – 0.355) less virulent on average compared to the
438 no-phage control populations (Figure 2b). In the control populations, 96 (80%) of the *G. mellonella*
439 died within 47 hours, with death occurring at a mean time of 19 hours. In contrast, only 32.5% and

440 41.2% of *G. mellonella* died in the phage added once and phage added repeatedly treatments
441 respectively, with a mean time to death of 36.7 and 35.4 hours (Figure 2b).
442 This difference was driven by two impacts of phage application. First, there was a huge
443 reduction in virulence of bacteria that were resistant to both phages. When resistant to both phage,
444 virulence reduced by 95.69% compared to susceptible bacteria (median hazard ratio = 0.0431,
445 95%CI = 0.0139-0.122) and was 93.33% lower than bacteria resistant to only a single phage
446 (median hazard ratio = 0.0663, 95%CI = 0.0179-0.247; Figure 2c). Meanwhile, there was no
447 reduction in virulence for bacteria resistant to just a single phage (median hazard ratio = 0.653,
448 95%CI = 0.185 -2.09) when compared to phage susceptible bacteria. Second, even susceptible
449 bacteria became less virulent after phage application, with a 91.14% median hazard ratio = 0.0886,
450 95%CI = 0.0246-0.344) reduction in the phage added once treatment and an 80.7% reduction when
451 phage was added repeatedly (median hazard ratio = 0.193, 95%CI = 0.04-1.06; Figure 2c).

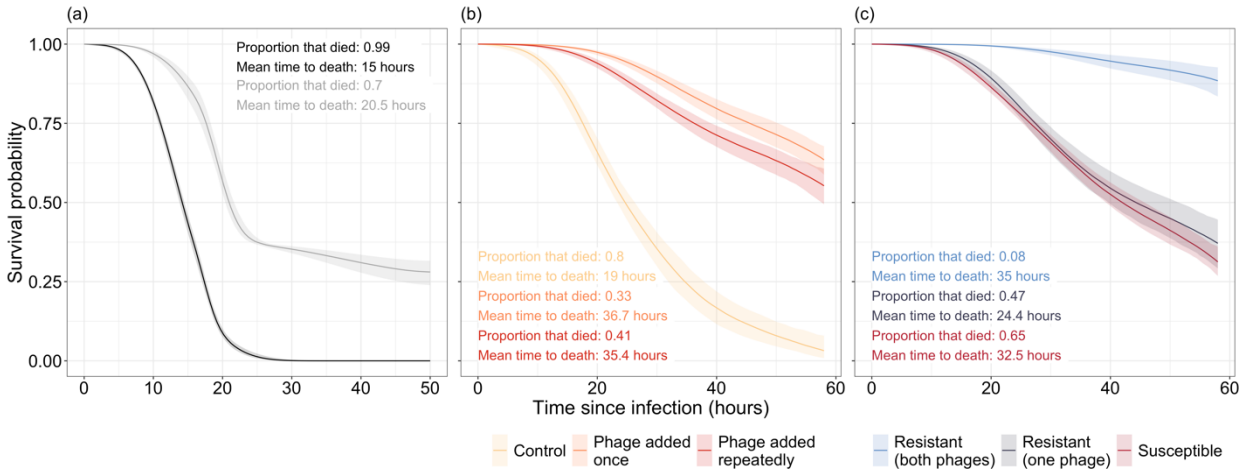

Figure 2. Survival curves of *G. mellonella* inoculated with *P. aeruginosa* isolates isolated (a) *in vivo* and (b, c) *in vitro*. (a) Virulence of bacterial isolates isolated from before (black) and after (grey) phage therapy. (b) Virulence of bacterial in control populations where no phage is present (yellow) is much greater than populations which were exposed to either a single (orange) or repeated (red) phage applications. (c) Virulence is significantly reduced in bacterial isolates resistant to both phages while bacteria resistant to one phage are non-significantly different in virulence to phage susceptible isolates. Lines represent the average prediction and shaded bands represent the 95% credible intervals of those predictions. Proportion and mean time to death of *Galleria* that died are presented as summary statistics for each treatment.

461

462 **Growth rate**

463 Evolving resistance against phage can trade-off with growth rates (Buckling et al., 2006; Koskella
464 et al., 2011; Wright et al., 2018), and could be a plausible mechanism for virulence reduction. In
465 the case of the *in vivo* isolates, the growth rate of pre-phage treatment isolates ($\bar{x}$ = 0.36, 95%CI =
466 0.342 - 0.369) was significantly higher than that of post-treatment isolates ($\bar{x}$ = 0.25, 95%CI =
467 0.195 - 0.302). Post-treatment isolates which evolved resistance (to one or both phage) had a
468 significantly lower growth rate ($\bar{x}$ = 0.21, 95%CI = 0.162 - 0.266) than the ancestral isolates ($\bar{x}$ =
469 0.36, 95%CI = 0.342 - 0.369). However, the 95% CIs of the susceptible isolates' growth rate ($\bar{x}$ =
470 0.33, 95%CI = 0.256 - 0.402) overlapped with the ancestral and resistant isolates, indicating non-
471 significance, which was likely driven by a lack of statistical power (n = 3 susceptible isolates)
472 (Figure 3a).

473 For *in vitro* isolates, growth rate was significantly affected by treatment (χ^2_2 = 20.14, p <
474 0.001) with the control group having significantly higher growth rates ($\bar{x}$ = 0.43, 95%CI = 0.373 -
475 0.477) compared to treatments in which phage were added once ($\bar{x}$ = 0.30, 95%CI = 0.256 - 0.346;
476 p = 0.002) or repeatedly ($\bar{x}$ = 0.276, 95%CI = 0.235 - 0.318; p < 0.001; Figure 3b). No significant
477 difference was observed in growth rates between each phage treatment (Tukey HSD: estimate =
478 0.025, t-ratio = 0.95, p = 0.628); and changes in growth were not associated with phage resistance
479 (interaction between treatment and resistance: χ^2_2 = 0.37, p = 0.832; fixed effect of resistance: χ^2_2 =
480 2.98, p = 0.226; Figure 3b).

481

482

483

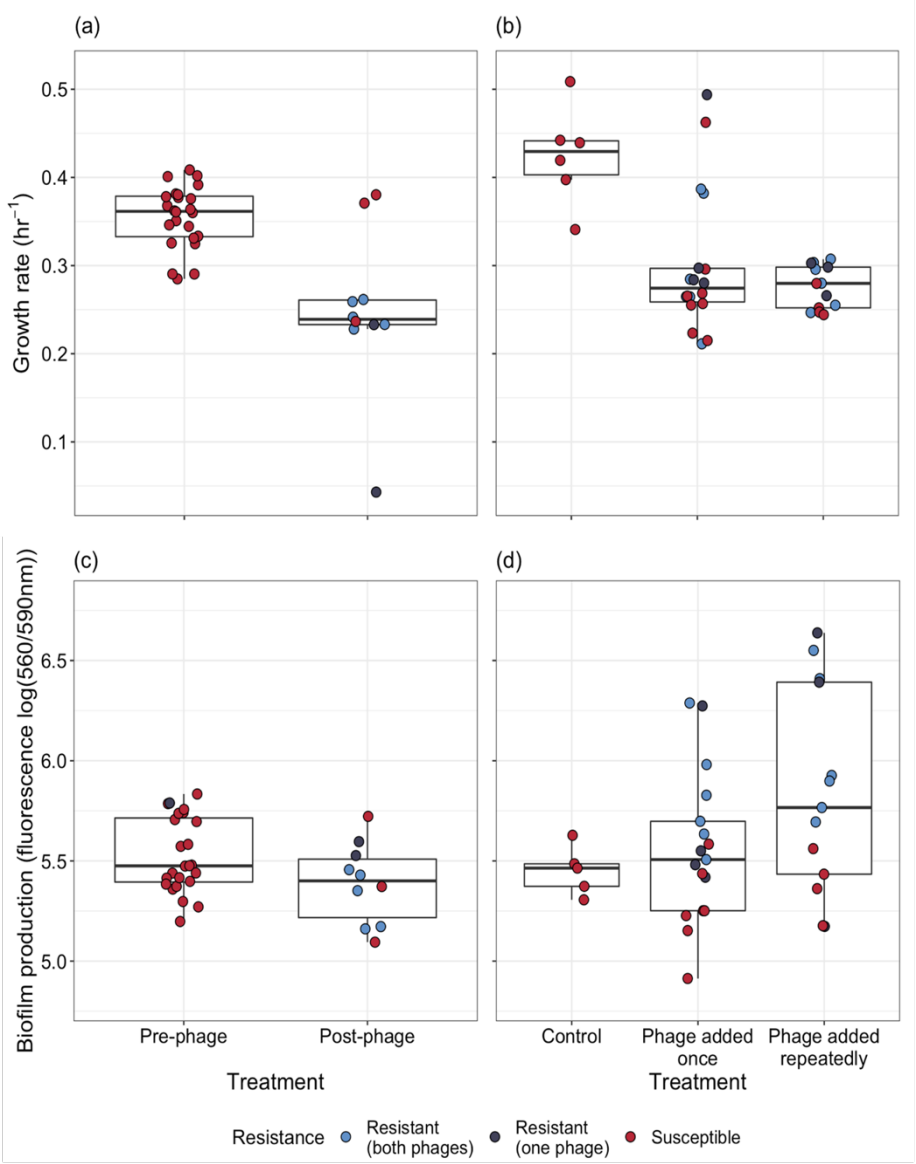

Figure 3. Phenotypic changes underpinning the resistance – virulence trade-off of bacterial populations. Populations were evolved (a, c) *in vivo*, and (b, d) *in vitro*. (a, b) Changes in bacterial growth were estimated for populations isolated (a) before and after phage treatment, and (b) between control and the phage treatment groups. Single points represent individual bacterial isolates of differing phage resistance levels: resistant to both phage (light blue), resistant to 14-1 or PNM (dark blue) or phage susceptible (red). Tops and bottoms of the bars represent the 75th and 25th percentiles of the data, the middle lines are the medians, and the whiskers extend from their respective hinge to the smallest or largest value no further than 1.5* interquartile range.

509

510 **Biofilm production**

511 Biofilm production is often altered in phage resistant isolates (Harrison et al., 2015; Kim et al.,
512 2015; Scanlan and Buckling, 2012) and this can also affect virulence and growth rate (Li et al.,
513 2008; Wang et al., 2011). Therefore, we compared the biofilm productivity between isolates
514 evolved *in vitro* and *in vivo*. For *in vivo* isolates, there was no significant difference in biofilm
515 production between isolates isolated pre- ($\bar{x}$ = 5.53, 95%CI = 5.45 - 5.6) or post-phage therapy
516 ($\bar{x}$ = 5.39, 95%CI = 5.27 – 5.5), and between phage resistant ($\bar{x}$ = 5.38, 95%CI = 5.27 – 5.50) and
517 susceptible isolates ($\bar{x}$ = 5.39, 95%CI = 5.1 – 5.69; Figure 3c).

518 For *in vitro* isolates, there was no significant difference in biofilm production between
519 treatments (treatment x resistance interaction: χ^2_2 = 0.785, p = 0.675; treatment: χ^2_2 = 4.52, p =
520 0.104). However, phage resistance was associated with increased biofilm production (χ^2_2 = 19.12,
521 p < 0.001), with phage susceptible isolates ($\bar{x}$ = 5.35, 95%CI = 5.16 – 5.54) having lower biofilm
522 production than isolates resistant to one ($\bar{x}$ = 5.85, 95%CI = 5.56 – 6.13; p = 0.012) or both phages
523 ($\bar{x}$ = 5.93, 95%CI = 5.73 – 6.13; p = 0.004; Figure 3d).

524

525 **Genetic basis of evolutionary changes**

526 Given the parallel phenotypic differences we observed under *in vivo* and *in vitro* conditions, we
527 next explored whether the underlying genetic changes were the same for *in vitro* and *in vivo*
528 evolved populations. From the *in vitro* pooled sequencing, we found significant changes in 27
529 different genes with known function (Figure 4), 15 of which were changes in frequency compared
530 to the ancestral population while 12 were novel mutations.

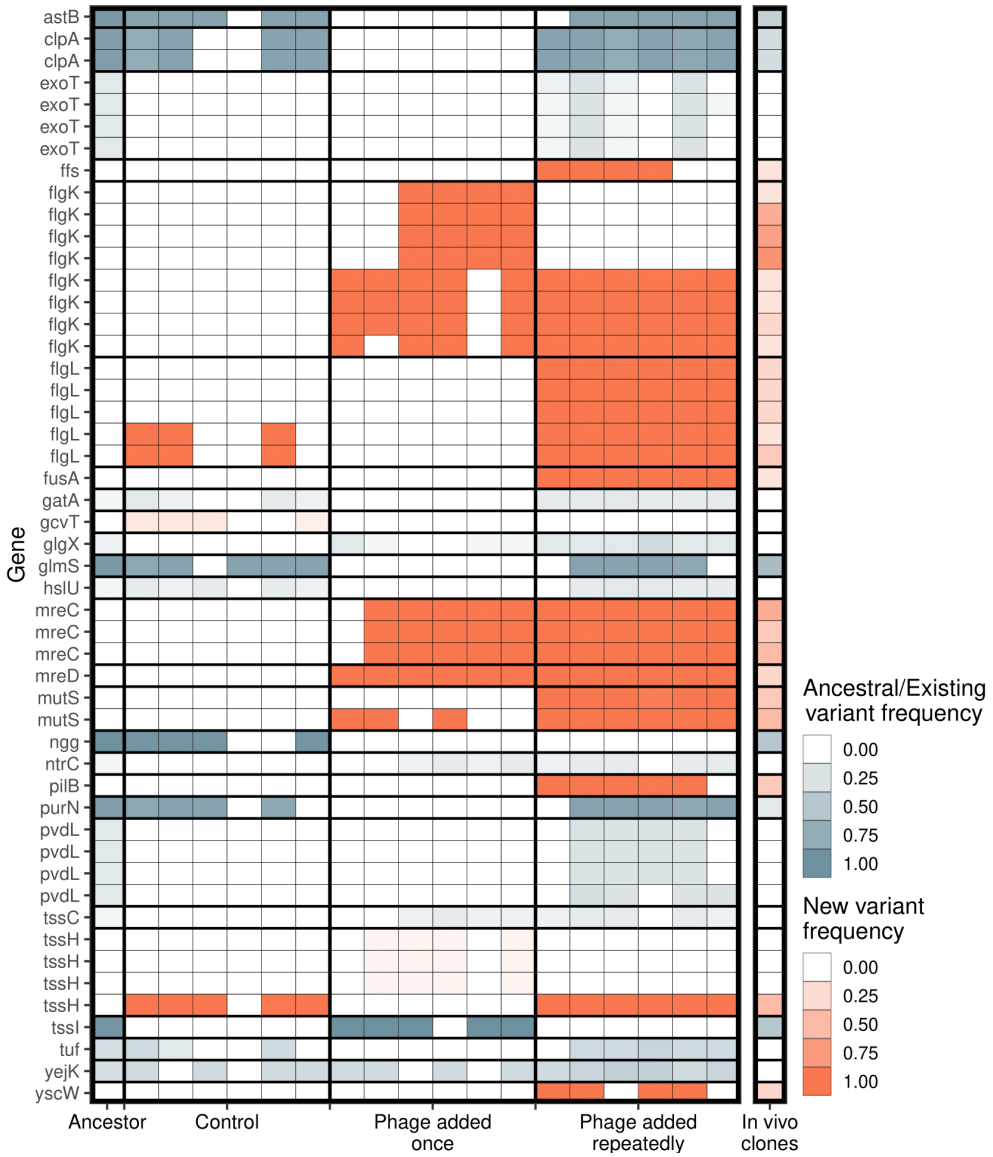

Figure 4. Significant genetic changes identified *in vitro* and *in vivo*. The frequency of genes that differed significantly between treatments *in vitro* are shown. Genetic changes that were already present in the ancestral population (first column) are shown in blue, while *de novo* mutations are in orange. Only genes whose function was identified are included. Multiple rows of the same gene indicate different genomic variants of the same gene. Colour intensity shows how frequent the genetic change is in the population. For *in vitro* treatments, each column is an independent replicate representing the results of the pooled sequencing. For the *in vivo* isolates (final column), all isolates were pooled to visualise the frequency of each genetic change *in vivo*.

540

541 In terms of genetic distance from the ancestral population, populations in the treatment
542 where phage was added repeatedly diverged more than when phage was added once (Tukey HSD:
543 t = -4.32, d.f. = 15, p = 0.0017), which diverged more from the ancestral populations than the
544 control populations (Tukey HSD: t = -8.81, d.f. = 15, p < 0.0001; Figure 5a, b). Consistent with
545 this, more novel SNPs/indels were found in the treatment populations where phages were added
546 repeatedly (mean = 19.2) compared to where phages were added once (mean = 11.8, Tukey HSD:
547 t = -4.80, d.f. = 15, p = 0.0006), which in turn had more novel SNPs/indels than control populations
548 (mean = 2.5, Tukey HSD: t = -6.105, d.f. = 15, p = 0.0001; Figure 5b). Within-population diversity
549 was highest in phage added repeatedly treatment (Tukey HSD phage added repeatedly *vs.* phage
550 added once: t = -5.96, d.f. = 15, p = 0.0001; Tukey HSD phage added repeatedly *vs.* control: t = -
551 4.33, d.f. = 15, p = 0.0016), but there was no difference between control populations and phage
552 added once treatment (Tukey HSD: t = -1.14, d.f. = 15, p = 0.2625; Figure 5c).

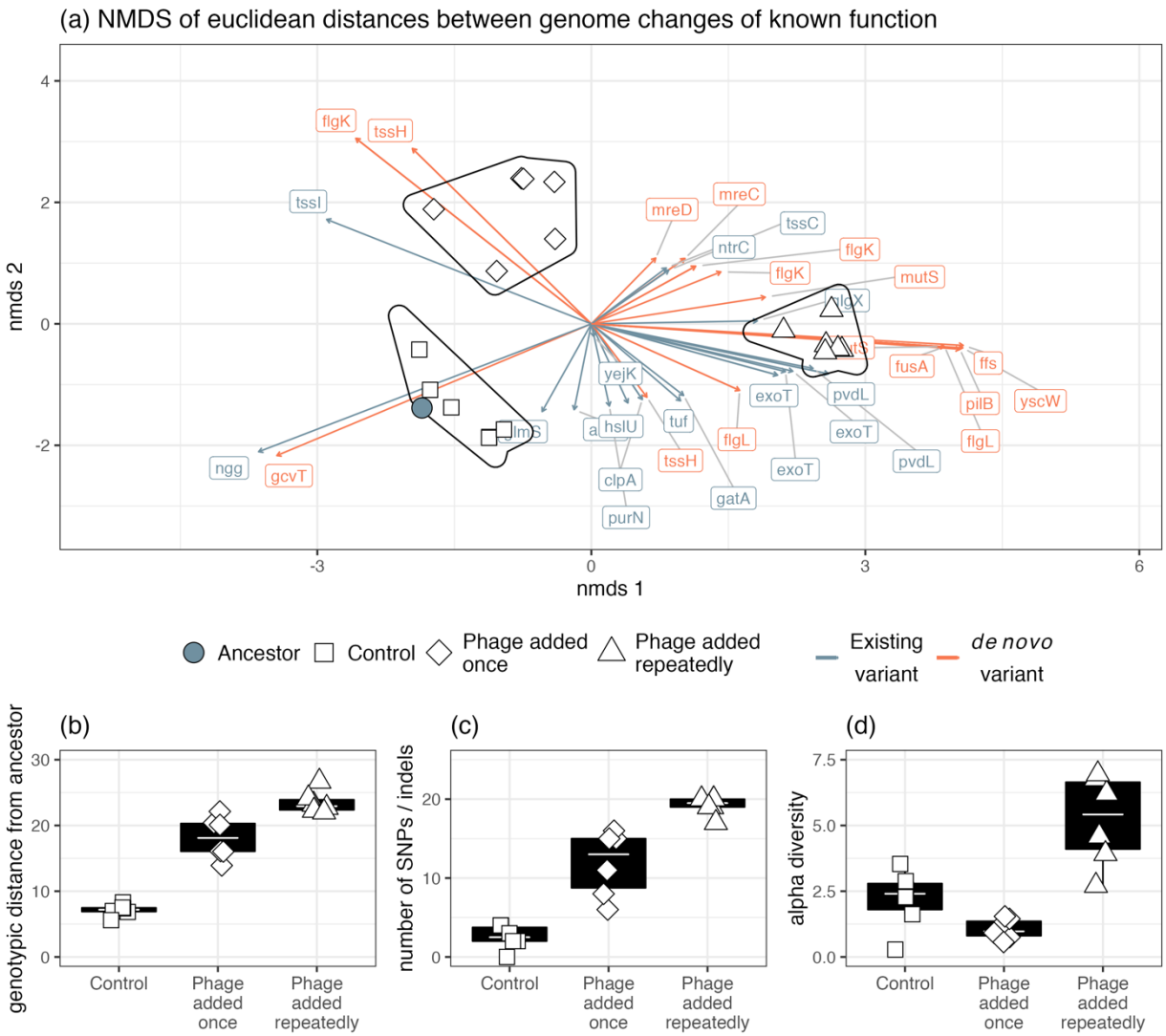

553

554 **Figure 5. Genomic changes for populations evolved *in vitro*.** (a) The divergence of each treatment group

555 as indicated by Euclidean distances of each gene from the ancestral isolates. Genetic changes were

556 characterised as a change in frequency of an existing gene in the ancestor or selection on a mutation that

557 was gained during experimental evolution. The presence of phage significantly affected (b) genotypic

558 distance from the ancestor, (c) the number of new SNPs and (d) alpha diversity.

559

560 *In vitro* treatment significantly altered genetic composition (i.e. the centroids of phage
561 added once, phage added repeatedly and control populations were different, Figure 4,
562 PERMANOVA, $F_{3,15} = 16.05$, $R^2 = 0.76$, $p = 0.0001$). There was no difference in beta-diversity
563 (calculated from distance-to-centroids between groups) between treatments (homogeneity of
564 multi-variation dispersion ANOVA: $F_{3,15} = 1.65$, $p = 0.22$). Genetic changes associated with both
565 *in vitro* phage treatments, but not control, were flagellar hook-associated protein (*flgK*) and rod-
566 shape determining proteins (*mreC* and *mreD*) (Figure 4). Additionally, genetic changes in DNA
567 mismatch repair (*mutS*), elongation factor G (*fusA*), signal recognition particle (*ffs*), type 3
568 secretion system pilotin (*yscW*), and pilus assembly protein (*pilB*) were mainly found *in vitro* in
569 the phage added repeatedly treatment (Figure 4). We examined whether these same mutations
570 arose in the clonal *in vivo* isolates. Of the 50 genetic changes identified *in vitro*, the *in vivo* isolates
571 had a mean of 11.8 changes (maximum = 23, minimum = 1). Changes in frequencies or mutations
572 were found at 16/27 of the same genes identified *in vitro* in at least one isolate (Figure 4). Crucially,
573 some of the *de novo* mutations that were at high frequency in vitro were also at high frequency in
574 vivo (*flgL* = 30%, *mutS* = 45%, *mreC* = 50%, *mreD* = 30%, *pilB* = 40%). We next assessed whether
575 mutations arising in individual isolates *in vivo* could be linked to phenotypic changes (resistance,
576 virulence, biofilm productivity, growth rate). If strong genotypic – phenotype links can be made,
577 we would expect isolates to cluster according to their trait value. However, we found no obvious
578 genotype to phenotype links *in vivo* and due to the small number of isolates, we were unable to
579 conduct robust statistical analyses (Figure S2).

580

581 **Discussion**

582 Highly parallel evolutionary dynamics were found *in vivo* and *in vitro*, showing that laboratory
583 studies can be predictive of clinical phage therapy (phage-mediated decolonisation). Levels of
584 phage resistance were comparable *in vivo* and *in vitro* with limited phage infectivity evolution
585 occurring only *in vitro*. Additionally, phage resistance was associated with trade-offs with
586 virulence and bacterial growth and similar mutations or genetic variants could explain these
587 parallel evolutionary changes in both ecological contexts.

588 Parallel evolution is promising for future clinical work in which the trajectory of bacteria
589 and phage (co)evolution may be predicted for individual patients. Given the difference in
590 environments between that of a laboratory and human nasal cavity, it was surprising that evolution
591 was so similar. The nasal cavity would have been more nutrient limited and spatially heterogenous
592 and such conditions have been shown to change bacteria – phage interactions compared to
593 evolution in laboratory growth medium. For instance, bacteria – phage coevolution is altered in
594 soil compared to growth medium because of increased costs of resistance in the former (Gomez
595 and Buckling, 2011); and in plant leaves, bacteria and phage have failed to evolve while otherwise
596 coevolving in the laboratory due to lower bacteria – phage contact rates (Hernandez and Koskella,
597 2019).

598 Rapid phage resistance has been highlighted as a concern for phage therapy development
599 (Torres-Barceló, 2018) and was found in this case study. Without ongoing reciprocal phage
600 evolution, phage resistance is likely to lead to regrowth of bacteria during infections; this has been
601 found in a few case studies but has been combatted by selecting a different phage (single or
602 cocktail) (Aslam et al., 2020; Schooley et al., 2017; Wu et al., 2021; Zhvania et al., 2017). That
603 resistance emerged predominantly by *de novo* mutations and not selection on existing variation
604 further highlights the fact that stressful *in vivo* conditions need not prevent bacteria from rapidly

605 adapting to phage. However, phage resistance was found to have growth rate costs which may
606 further explain why some isolates remained sensitive to phage, and why decolonisation was
607 ultimately successful. The natural nasal microbiota may have further contributed to this success
608 by outcompeting slower growing phage resistant isolates (Wang et al., 2019). Such resistance –
609 virulence trade-offs have been found in previous *in vitro*, animal model and clinical studies and is
610 expected to improve treatment success in spite of phage resistance (Oechslin, 2018). Phage
611 resistance however is not always costly and likely depends on the genetic background of the
612 bacteria and phage, as well as the environmental context (Meaden et al., 2015; van Houte et al.,
613 2016). The absence of clear links between resistance phenotypes and growth rate within our *in*
614 *vitro* treatments, despite clear between-treatment effects, is presumably because the cultures were
615 initiated with genetically diverse clinical isolates, rather than a single ancestral clone. Ultimately,
616 phage resistance was beneficial in controlling the pathogen in this case study and such benefits
617 could have led to treatment success.

618 Population genomics of the isolates *in vivo* and *in vitro* revealed parallel genomic changes
619 and the effects of phage selection at a molecular level. In line with previous studies, phage selection
620 accelerated molecular evolution which resulted in populations being more diverged from their
621 ancestral pool than control isolates (*in vitro*) (Morgan et al., 2010; Pal et al., 2007). This suggests
622 that phage placed strong selection on bacteria and this further resulted in mutator strains (*mutS*
623 genotype), especially where phage were added repeatedly *in vitro* and *in vivo*, that likely
624 accelerated the rate of evolution further (Morgan et al., 2010). Between both *in vivo* and *in vitro*
625 results, mutations selected by phage gave insight into potential mechanisms of resistance. In
626 particular, mutations to *mreD* and *mreC* encoded for cell shape (Cabeen and Jacobs-Wagner, 2005)
627 while missense mutations at *flgK* and *flgL* probably resulted in flagella loss (Macnab, 2003). The

628 result of these mutations was likely reduced cell surface area which reduces the probability of
629 phage absorption (Dennehy and Abedon, 2021). *pilB* mutations were also selected which is likely
630 a surface mutation to prevent PNM (a pilus binding phage) from attaching (Ceyssens et al., 2011).

631 Strong genotype – phenotype links were difficult to distinguish as a high number of the
632 same mutations or existing variants were selected upon both *in vivo* and *in vitro*, and no unique
633 candidate genes were obvious to explain phenotypic differences (i.e. growth rate, biofilm
634 production). Flagella and *mreC* mutations are associated with increased biofilm production
635 (Whiteley et al., 2001) and as they were found in the *in vitro* isolates, this may suggest a
636 generalistic phage defence strategy (Harper et al., 2014). However, as these same mutations were
637 found *in vivo*, without increases in biofilm production, strong genotype – phenotype links are
638 unclear. Surface mutation is a common form of phage resistance (van Houte et al., 2016) but here
639 it appears coupled with mechanisms that prevent absorption more generally; combined, these
640 strategies could have reduced bacterial growth and/or virulence by impairing swarming motility
641 (Haiko and Westerlund-Wikström, 2013). In contrast, other studies using the same phage but *P.*
642 *aeruginosa* PA01 instead reported mutations predominantly at pilus and lipopolysaccharide
643 receptors, showing that greater selection is placed on specific phage resistance strategies at phage
644 binding sites (Wright et al., 2019, 2018). Our results highlight the importance of genetic
645 background, and hence the use of clinical isolates over laboratory clones, in determining
646 evolutionary trajectories (Betts et al., 2014; Friman et al., 2016; León and Bastías, 2015; Rossitto
647 et al., 2018; van Houte et al., 2016).

648 How phages were applied *in vitro* had an impact on phage resistance. Although we
649 observed a greater number of mutations where phages were added repeatedly (mimicking multiple
650 phage doses), the proportion of resistant bacteria at the end of the experiment was significantly

651 lower (61.5%) compared to where phages were just added at the start of the experiment (90%).
652 That resistance of evolved bacteria to the ancestral phages (~90%) did not differ between
653 treatments suggests that differences in resistance to evolved phages was caused by phage
654 infectivity evolution in the repeated phage treatment. This infectivity evolution occurred before
655 the first time point, with no subsequent changes, and was presumably the result of greater mutation
656 supply rate in this repeated phage application treatment. Multiple (Manohar et al., 2018) and higher
657 (Barrow et al., 1998; Biswas et al., 2002; Debarbieux et al., 2010; Merril et al., 1996; Sunagar et
658 al., 2010; Vinodkumar et al., 2008; Wang et al., 2006; Wills et al., 2005) phage doses have been
659 shown previously to decrease morbidity and mortality in animal models. Our results build upon
660 this work to show that maintaining high phage titres may have a positive effect in reducing resistant
661 populations despite increasing the strength of selection for resistance.

662 Although our results suggest that results of laboratory studies may parallel phage resistance
663 – virulence trade-offs during *in vivo* phage therapy, there a number of important caveats. Firstly,
664 our *in vitro* – *in vivo* results were comparable with regards to the direction of change, but absolute
665 effect sizes were greater *in vitro*. For instance, we observed a higher proportion of phage resistant
666 isolates *in vitro* that were also far less virulent than isolates found *in vivo*. Therefore, it may be
667 expected that phenotypic changes will be exaggerated *in vitro*. Secondly, as this patient had a nasal
668 colonization, the role of the adaptive immune system would have been heavily reduced (Ooi et al.,
669 2008). The immune system has the potential to improve phage therapy success by synergistically
670 killing bacteria with phage which may diminish the potential for phage resistance by reducing
671 bacterial growth (Leung and Weitz, 2017; Roach et al., 2017). Alternatively, immune cells may
672 kill phage and therefore prevent phage acting on bacterial populations (Van Belleghem et al.,
673 2018). Additionally, the nasal cavity has a diverse microbiome that may have contributed to *P.*

674 *aeruginosa* decolonisation (Hu et al., 2018; Kumpitsch et al., 2019). The role of the microbiome
675 will differ in infection type, with gut and respiratory infections potentially having a greater
676 microbiome effect (Hu et al., 2018; Kumpitsch et al., 2019; Lloyd-Price et al., 2016) while septic
677 infections may have a greater immune system effect (Van Belleghem et al., 2018). Therefore, it is
678 important to compare laboratory vs *in vivo* phage therapy in a number of infection types. The
679 genomic background of the bacteria may further affect how sensitive its resistance strategies are
680 to the environment it is in as more costly resistance strategies are more likely to be selected *in vitro*
681 than *in vivo* (van Houte et al., 2016). This encompasses not only genetic variation within species
682 but also differences between species that may differ in infection sites, immune responses, virulence
683 and sensitivity to phage (Abedon, 2019; Doffkay et al., 2015; van Houte et al., 2016). Further work
684 using isolates from case studies and clinical trials will give an insight into the predictability of
685 bacteria and phage evolution from laboratory to *in vivo* studies.
686

687 **References**

688 Abedon, S.T., 2019. Use of phage therapy to treat long-standing, persistent, or chronic
689 bacterial infections. Adv. Drug Deliv. Rev. 145, 18–39.
690 https://doi.org/10.1016/j.addr.2018.06.018
691 Abedon, S.T., 2017. Information Phage Therapy Research Should Report. Pharmaceuticals 10,
692 43. https://doi.org/10.3390/ph10020043
693 Aslam, S., Lampley, E., Wooten, D., Karris, M., Benson, C., Strathdee, S., Schooley, R.T.,
694 2020. Lessons Learned From the First 10 Consecutive Cases of Intravenous
695 Bacteriophage Therapy to Treat Multidrug-Resistant Bacterial Infections at a Single
696 Center in the United States. Open Forum Infect. Dis. 7, ofaa389.
697 https://doi.org/10.1093/ofid/ofaa389
698 Barrow, P., Lovell, M., Berchieri, A., 1998. Use of lytic bacteriophage for control of experimental
699 Escherichia coli septicemia and meningitis in chickens and calves. Clin. Diagn. Lab.
700 Immunol. 5, 294–298.
701 Bates, D., Maechler, M., Bolker, B., Walker, S., 2014. lme4: Linear mixed-effects models using
702 Eigen and S4. R Package Version.
703 Betts, A., Kaltz, O., Hochberg, M.E., 2014. Contrasted coevolutionary dynamics between a
704 bacterial pathogen and its bacteriophages. Proc. Natl. Acad. Sci. U.S.A. 111, 11109–
705 11114. https://doi.org/10.1073/pnas.1406763111
706 Biswas, B., Adhya, S., Washart, P., Paul, B., Trostel, A.N., Powell, B., Carlton, R., Merril, C.R.,
707 2002. Bacteriophage Therapy Rescues Mice Bacteremic from a Clinical Isolate of

Vancomycin-Resistant Enterococcus faecium. Infect. Immun. 70, 204–210. https://doi.org/10.1128/IAI.70.1.204-210.2002

Brix, A., Cafora, M., Aureli, M., Pistocchi, A., 2020. Animal Models to Translate Phage Therapy to Human Medicine. Int J Mol Sci 21, 3715. https://doi.org/10.3390/ijms21103715

Buckling, A., Rainey, P.B.., 2002. Antagonistic coevolution between a bacterium and a bacteriophage. Proc. Royal Soc. B 269, 931–936. https://doi.org/10.1098/rspb.2001.1945

Buckling, A., Wei, Y., Massey, R.C., Brockhurst, M.A., Hochberg, M.E., 2006. Antagonistic coevolution with parasites increases the cost of host deleterious mutations. Proc. Royal Soc. B 273, 45–49. https://doi.org/10.1098/rspb.2005.3279

Cabeen, M.T., Jacobs-Wagner, C., 2005. Bacterial cell shape. Nat Rev Microbiol 3, 601–610. https://doi.org/10.1038/nrmicro1205

Canty, A., Ripley, B., 2021. boot: Bootstrap Functions.

Ceyssens, P.-J., Glonti, T., Kropinski, ndrew M., Lavigne, R., Chanishvili, N., Kulakov, L., Lashkhi, N., Tediashvili, M., Merabishvili, M., 2011. Phenotypic and genotypic variations within a single bacteriophage species. Virol J 8, 134. https://doi.org/10.1186/1743-422X-8-134

Debarbieux, L., Leduc, D., Maura, D., Morello, E., Criscuolo, A., Grossi, O., Balloy, V., Touqui, L., 2010. Bacteriophages Can Treat and Prevent *Pseudomonas aeruginosa* Lung Infections. J Infect Dis 201, 1096–1104. https://doi.org/10.1086/651135

Dennehy, J.J., Abedon, S.T., 2021. Adsorption: Phage Acquisition of Bacteria, in: Harper, D.R., Abedon, S.T., Burrowes, B.H., McConville, M.L. (Eds.), Bacteriophages. Springer International Publishing, Cham, pp. 93–117. https://doi.org/10.1007/978-3-319-41986-2_2

Doffkay, Z., Dömötör, D., Kovács, T., Rákhely, G., 2015. Bacteriophage therapy against plant, animal and human pathogens. Acta Biol. Szeged. 59, 291–302.

Edgeworth, J.D., 2011. Has decolonization played a central role in the decline in UK methicillin-resistant Staphylococcus aureus transmission? A focus on evidence from intensive care. Journal of Antimicrobial Chemotherapy 66, ii41–ii47. https://doi.org/10.1093/jac/dkq325

Everest, P., 2007. Stress and bacteria: microbial endocrinology. Gut 56, 1037–1038. https://doi.org/10.1136/gut.2006.117150

Friman, V.-P., Soanes-Brown, D., Sierocinski, P., Molin, S., Johansen, H.K., Merabishvili, M., Pirnay, J.-P., De Vos, D., Buckling, A., 2016. Pre-adapting parasitic phages to a pathogen leads to increased pathogen clearance and lowered resistance evolution with *Pseudomonas aeruginosa* cystic fibrosis bacterial isolates. J. Evol. Biol. 29, 188–198. https://doi.org/10.1111/jeb.12774

Gandon, S., Buckling, A., Decaestecker, E., Day, T., 2008. Host-parasite coevolution and patterns of adaptation across time and space. J. Evol. Biol. 21, 1861–1866. https://doi.org/10.1111/j.1420-9101.2008.01598.x

Gomez, P., Buckling, A., 2011. Bacteria-Phage Antagonistic Coevolution in Soil. Science 332, 106–109. https://doi.org/10.1126/science.1198767

Goodrich, B., 2020. rstanarm: Bayesian Applied Regression Modeling via Stan.

Górski, A., Dąbrowska, K., Hodyra-Stefaniak, K., Borysowski, J., Międzybrodzki, R., Weber-Dąbrowska, B., 2015. Phages targeting infected tissues: novel approach to phage therapy. Future Microbiol. 10, 199–204. https://doi.org/10.2217/fmb.14.126

Haiko, J., Westerlund-Wikström, B., 2013. The Role of the Bacterial Flagellum in Adhesion and Virulence. Biology 2, 1242–1267. https://doi.org/10.3390/biology2041242

Hampton, H.G., Watson, B.N.J., Fineran, P.C., 2020. The arms race between bacteria and their phage foes. Nature 577, 327–336. https://doi.org/10.1038/s41586-019-1894-8

757 Harper, D., Parracho, H., Walker, J., Sharp, R., Hughes, G., Werthén, M., Lehman, S., Morales,
758 S., 2014. Bacteriophages and Biofilms. Antibiotics 3, 270–284.
759 https://doi.org/10.3390/antibiotics3030270
760 Harrison, E., Truman, J., Wright, R., Spiers, A.J., Paterson, S., Brockhurst, M.A., 2015. Plasmid
761 carriage can limit bacteria–phage coevolution. Biol. Lett. 11, 20150361.
762 https://doi.org/10.1098/rsbl.2015.0361
763 Hernandez, C.A., Koskella, B., 2019. Phage resistance evolution *in vitro* is not reflective of *in*
764 *vivo* outcome in a plant-bacteria-phage system*. Evolution 73, 2461–2475.
765 https://doi.org/10.1111/evo.13833
766 Hu, Y.O.O., Hugerth, L.W., Bengtsson, C., Alisjahbana, A., Seifert, M., Kamal, A., Sjöling, Å.,
767 Midtvedt, T., Norin, E., Du, J., Engstrand, L., 2018. Bacteriophages Synergize with the
768 Gut Microbial Community To Combat *Salmonella*. mSystems 3, e00119-18,
769 /msystems/3/5/msys.00119-18.atom. https://doi.org/10.1128/mSystems.00119-18
770 Jariah, R.O.A., Hakim, M.S., 2019. Interaction of phages, bacteria, and the human immune
771 system: Evolutionary changes in phage therapy. Rev Med Virol 29.
772 https://doi.org/10.1002/rmv.2055
773 Kay, M., Mastny, T., 2020. tidybayes: Tidy Data and “Geoms” for Bayesian Models.
774 Kim, M.S., Kim, Y.D., Hong, S.S., Park, K., Ko, K.S., Myung, H., 2015. Phage-Encoded Colanic
775 Acid-Degrading Enzyme Permits Lytic Phage Infection of a Capsule-Forming Resistant
776 Mutant Escherichia coli Strain. Appl. Environ. Microbiol. 81, 900–909.
777 https://doi.org/10.1128/AEM.02606-14
778 Koskella, B., Meaden, S., 2013. Understanding Bacteriophage Specificity in Natural Microbial
779 Communities. Viruses 5, 806–823. https://doi.org/10.3390/v5030806
780 Koskella, B., Taylor, T.B., Bates, J., Buckling, A., 2011. Using experimental evolution to explore
781 natural patterns between bacterial motility and resistance to bacteriophages. ISME J 5,
782 1809–1817. https://doi.org/10.1038/ismej.2011.47
783 Kropinski, A.M., Chan, L., Jarrell, K., Milazzo, F.H., 1977. The nature of *Pseudomonas*
784 *aeruginosa* strain PAO bacteriophage receptors. Can. J. Microbiol. 23, 653–658.
785 https://doi.org/10.1139/m77-098
786 Kumpitsch, C., Koskinen, K., Schöpf, V., Moissl-Eichinger, C., 2019. The microbiome of the
787 upper respiratory tract in health and disease. BMC Biol 17, 87.
788 https://doi.org/10.1186/s12915-019-0703-z
789 Kwiatek, M., Parasion, S., Nakonieczna, A., 2020. Therapeutic bacteriophages as a rescue
790 treatment for drug-resistant infections – an *in vivo* studies overview. J Appl Microbiol
791 128, 985–1002. https://doi.org/10.1111/jam.14535
792 Leitner, L., Ujmajuridze, A., Chanishvili, N., Goderdzishvili, M., Chkonia, I., Rigvava, S.,
793 Chkhotua, A., Changashvili, G., McCallin, S., Schneider, M.P., Liechti, M.D., Mehnert,
794 U., Bachmann, L.M., Sybesma, W., Kessler, T.M., 2021. Intravesical bacteriophages for
795 treating urinary tract infections in patients undergoing transurethral resection of the
796 prostate: a randomised, placebo-controlled, double-blind clinical trial. The Lancet
797 Infectious Diseases 21, 427–436. https://doi.org/10.1016/S1473-3099(20)30330-3
798 Lenth, R., 2018. Emmeans: Estimated marginal means, aka least-squares means. R Package
799 Version.
800 León, M., Bastías, R., 2015. Virulence reduction in bacteriophage resistant bacteria. Front.
801 Microbiol. 06. https://doi.org/10.3389/fmicb.2015.00343
802 Leung, C.Y. (Joey), Weitz, J.S., 2017. Modeling the synergistic elimination of bacteria by phage
803 and the innate immune system. J. Theor. Biol. 429, 241–252.
804 https://doi.org/10.1016/j.jtbi.2017.06.037
805 Li, L., Zhou, R., Li, T., Kang, M., Wan, Y., Xu, Z., Chen, H., 2008. Enhanced biofilm formation
806 and reduced virulence of Actinobacillus pleuropneumoniae luxS mutant. Microb. Pathog.
807 45, 192–200. https://doi.org/10.1016/j.micpath.2008.05.008

808 Lloyd-Price, J., Abu-Ali, G., Huttenhower, C., 2016. The healthy human microbiome. Genome
809 Med 8, 51. https://doi.org/10.1186/s13073-016-0307-y
810 Lopez Pascua, L., Hall, A.R., Best, A., Morgan, A.D., Boots, M., Buckling, A., 2014. Higher
811 resources decrease fluctuating selection during host-parasite coevolution. Ecol Lett 17,
812 1380–1388. https://doi.org/10.1111/ele.12337
813 Macnab, R.M., 2003. How Bacteria Assemble Flagella. Annu. Rev. Microbiol. 57, 77–100.
814 https://doi.org/10.1146/annurev.micro.57.030502.090832
815 Mainz, J.G., Naehrlich, L., Schien, M., Kading, M., Schiller, I., Mayr, S., Schneider, G.,
816 Wiedemann, B., Wiehlmann, L., Cramer, N., Pfister, W., Kahl, B.C., Beck, J.F., Tummler,
817 B., 2009. Concordant genotype of upper and lower airways P aeruginosa and S aureus
818 isolates in cystic fibrosis. Thorax 64, 535–540. https://doi.org/10.1136/thx.2008.104711
819 Mangalea, M.R., Duerkop, B.A., 2020. Fitness trade-offs resulting from bacteriophage
820 resistance potentiate synergistic antibacterial strategies. Infect Immun IAI.00926-19,
821 iai;IAI.00926-19v1. https://doi.org/10.1128/IAI.00926-19
822 Manohar, P., Nachimuthu, R., Lopes, B.S., 2018. The therapeutic potential of bacteriophages
823 targeting gram-negative bacteria using Galleria mellonella infection model. BMC
824 Microbiol 18. https://doi.org/10.1186/s12866-018-1234-4
825 Meaden, S., Paszkiewicz, K., Koskella, B., 2015. The cost of phage resistance in a plant
826 pathogenic bacterium is context-dependent. Evolution 69, 1321–1328.
827 https://doi.org/10.1111/evo.12652
828 Merabishvili, M., Pirnay, J.-P., Verbeken, G., Chanishvili, N., Tediashvili, M., Lashkhi, N., Glonti,
829 T., Krylov, V., Mast, J., Van Parys, L., Lavigne, R., Volckaert, G., Mattheus, W.,
830 Verween, G., De Corte, P., Rose, T., Jennes, S., Zizi, M., De Vos, D., Vaneechoutte, M.,
831 2009. Quality-Controlled Small-Scale Production of a Well-Defined Bacteriophage
832 Cocktail for Use in Human Clinical Trials. PLoS ONE 4, e4944.
833 https://doi.org/10.1371/journal.pone.0004944
834 Merril, C.R., Biswas, B., Carlton, R., Jensen, N.C., Creed, G.J., Zullo, S., Adhya, S., 1996.
835 Long-circulating bacteriophage as antibacterial agents. Proc. Natl. Acad. Sci. U.S.A. 93,
836 3188–3192. https://doi.org/10.1073/pnas.93.8.3188
837 MicrobesNG Sequencing Service Methods v20210419, n.d.
838 Morgan, A.D., Bonsall, M.B., Buckling, A., 2010. Impact of bacterial mutation rate on
839 coevolutionary dynamics between bacteria and phages. Evolution 64, 2980–7.
840 https://doi.org/10.1111/j.1558-5646.2010.01037.x
841 Morgan, A.D., Gandon, S., Buckling, A., 2005. The effect of migration on local adaptation in a
842 coevolving host–parasite system. Nature 437, 253–256.
843 https://doi.org/10.1038/nature03913
844 Oechslin, F., 2018. Resistance Development to Bacteriophages Occurring during Bacteriophage
845 Therapy. Viruses 10, 351. https://doi.org/10.3390/v10070351
846 Ooi, E.H., Wormald, P.-J., Tan, L.W., 2008. Innate Immunity in the Paranasal Sinuses: A
847 Review of Nasal Host Defenses. Am. J. Rhinol. 22, 13–19.
848 https://doi.org/10.2500/ajr.2008.22.3127
849 Pal, C., Maciá, M.D., Oliver, A., Schachar, I., Buckling, A., 2007. Coevolution with viruses drives
850 the evolution of bacterial mutation rates. Nature 450, 1079–1081.
851 https://doi.org/10.1038/nature06350
852 Peeters, E., Nelis, H.J., Coenye, T., 2008. Comparison of multiple methods for quantification of
853 microbial biofilms grown in microtiter plates. J. Microbiol. Methods 72, 157–165.
854 https://doi.org/10.1016/j.mimet.2007.11.010
855 Roach, D.R., Leung, C.Y., Henry, M., Morello, E., Singh, D., Di Santo, J.P., Weitz, J.S.,
856 Debarbieux, L., 2017. Synergy between the Host Immune System and Bacteriophage Is
857 Essential for Successful Phage Therapy against an Acute Respiratory Pathogen. Cell
858 Host & Microbe 22, 38-47.e4. https://doi.org/10.1016/j.chom.2017.06.018

859 Rossitto, M., Fiscarelli, E.V., Rosati, P., 2018. Challenges and Promises for Planning Future
860 Clinical Research Into Bacteriophage Therapy Against Pseudomonas aeruginosa in
861 Cystic Fibrosis. An Argumentative Review. Front. Microbiol. 9, 775.
862 https://doi.org/10.3389/fmicb.2018.00775
863 Scanlan, P.D., Buckling, A., 2012. Co-evolution with lytic phage selects for the mucoid
864 phenotype of Pseudomonas fluorescens SBW25. ISME J 6, 1148–1158.
865 https://doi.org/10.1038/ismej.2011.174
866 Scanlan, P.D., Buckling, A., Hall, A.R., 2015. Experimental evolution and bacterial resistance:
867 (co)evolutionary costs and trade-offs as opportunities in phage therapy research.
868 Bacteriophage 5, e1050153. https://doi.org/10.1080/21597081.2015.1050153
869 Schooley, R.T., Biswas, B., Gill, J.J., Hernandez-Morales, A., Lancaster, J., Lessor, L., Barr,
870 J.J., Reed, S.L., Rohwer, F., Benler, S., Segall, A.M., Taplitz, R., Smith, D.M., Kerr, K.,
871 Kumaraswamy, M., Nizet, V., Lin, L., McCauley, M.D., Strathdee, S.A., Benson, C.A.,
872 Pope, R.K., Leroux, B.M., Picel, A.C., Mateczun, A.J., Cilwa, K.E., Regeimbal, J.M.,
873 Estrella, L.A., Wolfe, D.M., Henry, M.S., Quinones, J., Salka, S., Bishop-Lilly, K.A.,
874 Young, R., Hamilton, T., 2017. Development and Use of Personalized Bacteriophage-
875 Based Therapeutic Cocktails To Treat a Patient with a Disseminated Resistant
876 Acinetobacter baumannii Infection. Antimicrob Agents Chemother 61, e00954-17,
877 e00954-17. https://doi.org/10.1128/AAC.00954-17
878 Sunagar, R., Patil, S.A., Chandrakanth, R.K., 2010. Bacteriophage therapy for Staphylococcus
879 aureus bacteremia in streptozotocin-induced diabetic mice. Res. Microbiol. 161, 854–
880 860. https://doi.org/10.1016/j.resmic.2010.09.011
881 Team, R.C., 2013. R: a language and environment for statistical computing.
882 Torres-Barceló, C., 2018. Phage Therapy Faces Evolutionary Challenges. Viruses 10, 323.
883 https://doi.org/10.3390/v10060323
884 Torres-Barceló, C., Hochberg, M.E., 2016. Evolutionary Rationale for Phages as Complements
885 of Antibiotics. Trends Microbiol. 24, 249–256. https://doi.org/10.1016/j.tim.2015.12.011
886 Tsai, C.J.-Y., Loh, J.M.S., Proft, T., 2016. *Galleria mellonella* infection models for the study of
887 bacterial diseases and for antimicrobial drug testing. Virulence 7, 214–229.
888 https://doi.org/10.1080/21505594.2015.1135289
889 Van Belleghem, J., Dąbrowska, K., Vaneechoutte, M., Barr, J., Bollyky, P., 2018. Interactions
890 between Bacteriophage, Bacteria, and the Mammalian Immune System. Viruses 11, 10.
891 https://doi.org/10.3390/v11010010
892 van Houte, S., Buckling, A., Westra, E.R., 2016. Evolutionary Ecology of Prokaryotic Immune
893 Mechanisms. Microbiol. Mol. Biol. Rev. 80, 745–763.
894 https://doi.org/10.1128/MMBR.00011-16
895 Vinodkumar, C., Kalsurmath, S., Neelagund, Y., 2008. Utility of lytic bacteriophage in the
896 treatment of multidrug-resistant *Pseudomonas aeruginosa* septicemia in mice. Indian J
897 Pathol Microbiol 51, 360. https://doi.org/10.4103/0377-4929.42511
898 Wang, J., Hu, B., Xu, M., Yan, Q., Liu, S., Zhu, X., Sun, Z., Tao, D., Ding, L., Reed, E., Gong, J.,
899 Li, Q.Q., Hu, J., 2006. Therapeutic effectiveness of bacteriophages in the rescue of mice
900 with extended spectrum beta-lactamase-producing Escherichia coli bacteremia. Int. J.
901 Mol. Med. 17, 347–355.
902 Wang, X., Wei, Z., Yang, K., Wang, J., Jousset, A., Xu, Y., Shen, Q., Friman, V.-P., 2019.
903 Phage combination therapies for bacterial wilt disease in tomato. Nat Biotechnol 37,
904 1513–1520. https://doi.org/10.1038/s41587-019-0328-3
905 Wang, Y., Zhang, W., Wu, Z., Lu, C., 2011. Reduced virulence is an important characteristic of
906 biofilm infection of Streptococcus suis: Biofilms of Streptococcus suis cause reduced
907 virluence. FEMS Microbiol. Lett. 316, 36–43. https://doi.org/10.1111/j.1574-
908 6968.2010.02189.x

Wertheim, H.F., Vos, M.C., Ott, A., van Belkum, A., Voss, A., Kluytmans, J.A., van Keulen, P.H., Vandenbroucke-Grauls, C.M., Meester, M.H., Verbrugh, H.A., 2004. Risk and outcome of nosocomial Staphylococcus aureus bacteraemia in nasal carriers versus non-carriers. The Lancet 364, 703–705. https://doi.org/10.1016/S0140-6736(04)16897-9

Whiteley, M., Bangera, M.G., Bumgarner, R.E., Parsek, M.R., Teitzel, G.M., Lory, S., Greenberg, E.P., 2001. Gene expression in Pseudomonas aeruginosa biofilms. Nature 413, 860–864. https://doi.org/10.1038/35101627

WHO, 2019. No time to wait: securing the future from drug-resistant infections. Report to the secretary-general of the United Nations. https://www.who.int/antimicrobial-resistance/interagency-coordination-group/IACG_final_report_EN.pdf?ua=1.

Wickham, H., 2016. ggplot2: elegant graphics for data analysis. Springer, New York.

Wills, Q.F., Kerrigan, C., Soothill, J.S., 2005. Experimental Bacteriophage Protection against Staphylococcus aureus Abscesses in a Rabbit Model. Antimicrob. Agents Chemother. 49, 1220–1221. https://doi.org/10.1128/AAC.49.3.1220-1221.2005

Wright, R.C.T., Friman, V.-P., Smith, M.C.M., Brockhurst, M.A., 2019. Resistance Evolution against Phage Combinations Depends on the Timing and Order of Exposure. mBio 10, e01652-19, /mbio/10/5/mBio.01652-19.atom. https://doi.org/10.1128/mBio.01652-19

Wright, R.C.T., Friman, V.-P., Smith, M.C.M., Brockhurst, M.A., 2018. Cross-resistance is modular in bacteria–phage interactions. PLoS Biol 16, e2006057. https://doi.org/10.1371/journal.pbio.2006057

Wu, N., Dai, J., Guo, M., Li, Jianhui, Zhou, X., Li, F., Gao, Y., Qu, H., Lu, H., Jin, J., Li, T., Shi, L., Wu, Q., Tan, R., Zhu, M., Yang, L., Ling, Y., Xing, S., Zhang, J., Yao, B., Le, S., Gu, J., Qin, J., Li, Jie, Cheng, M., Tan, D., Li, L., Zhang, Y., Zhu, Z., Cai, J., Song, Z., Guo, X., Chen, L.-K., Zhu, T., 2021. Pre-optimized phage therapy on secondary *Acinetobacter baumannii* infection in four critical COVID-19 patients. Emerg. Microbes Infect. 10, 612–618. https://doi.org/10.1080/22221751.2021.1902754

Zhvania, P., Hoyle, N.S., Nadareishvili, L., Nizharadze, D., Kutateladze, M., 2017. Phage Therapy in a 16-Year-Old Boy with Netherton Syndrome. Front. Med. 4, 94. https://doi.org/10.3389/fmed.2017.00094

Supplementary material

Parallel resistance evolution to phages during clinical phage therapy and in vitro

Supplementary figures

Data cleaning of the growth rate assays. As shown in Figure S1, we observed a sharp increase in OD_{600} reads within the initial 2.5 hours which was separate from the exponential growth phase. To prevent the rolling regression taking these initial measurements into account, these values were removed from analyses.

(a) Replicate 1

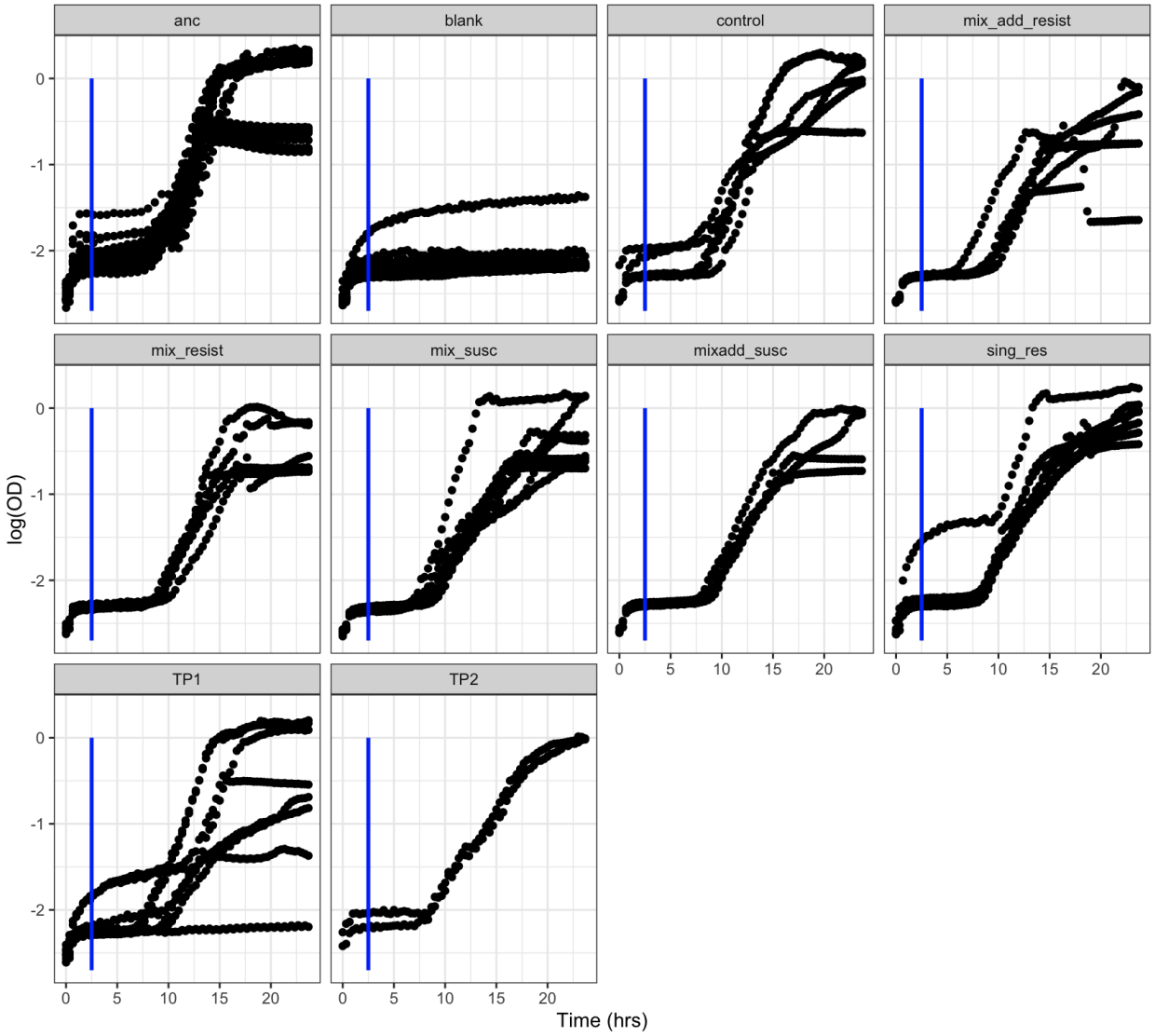

(b) Replicate 2

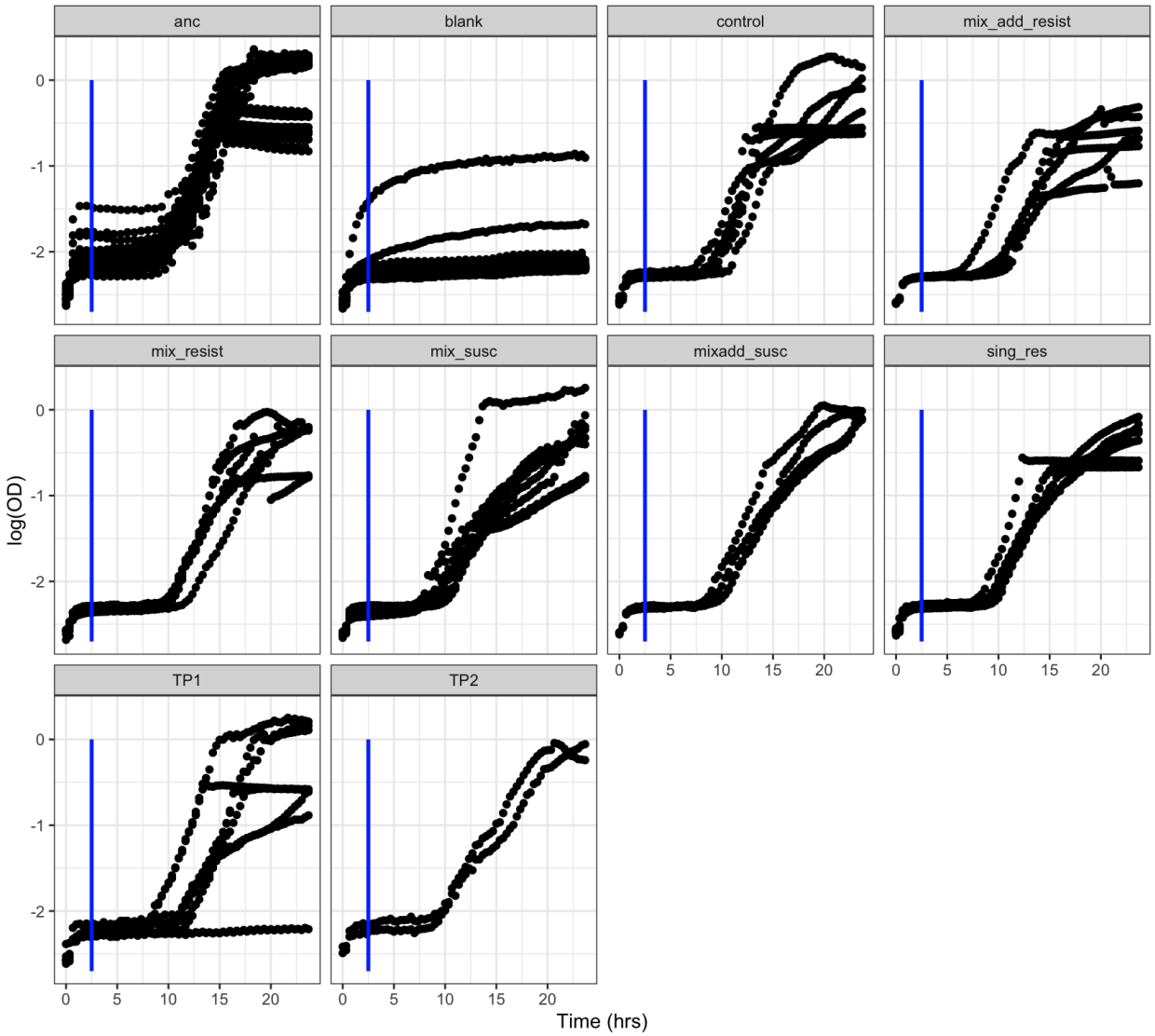

(c) Replicate 3

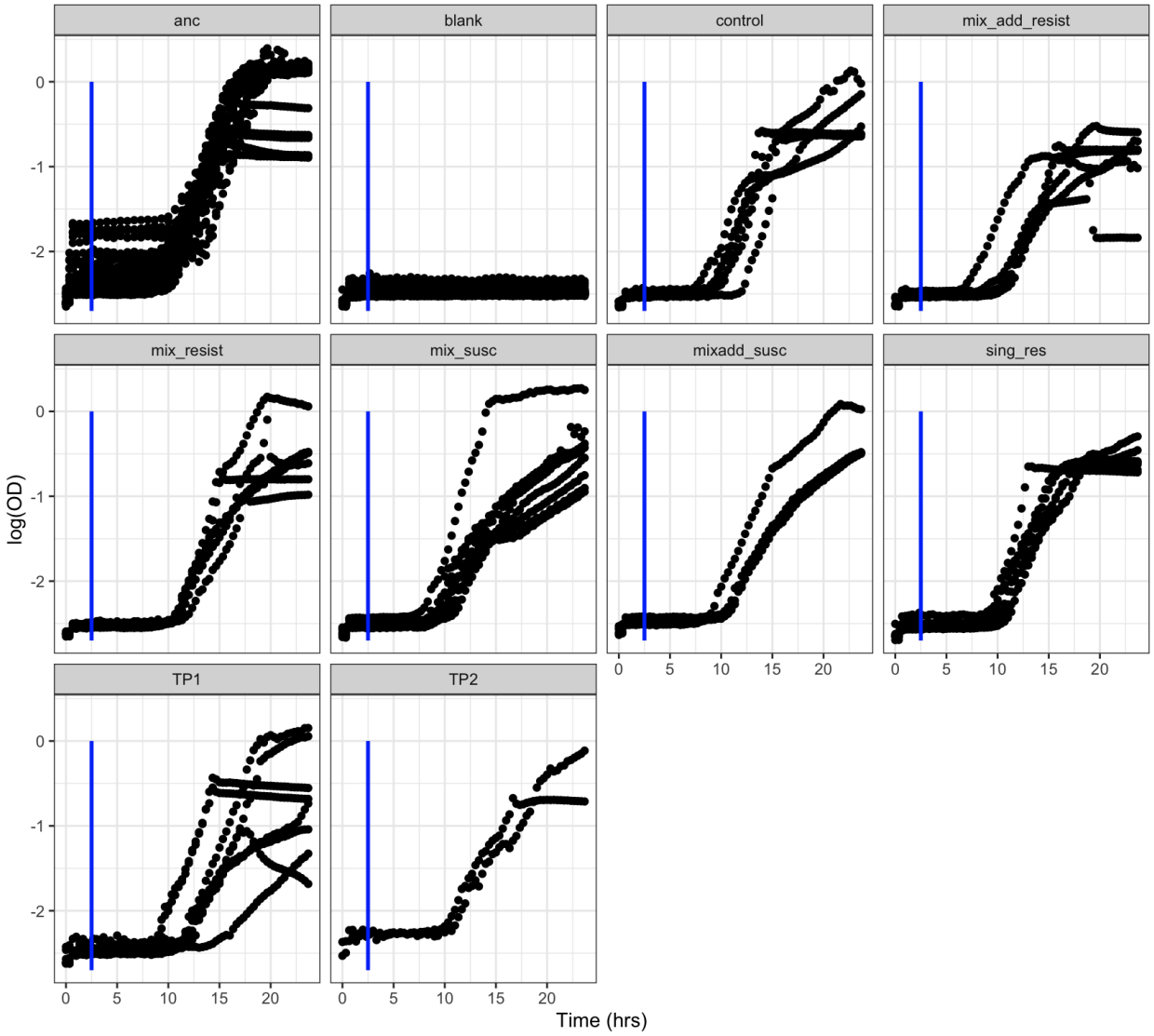

Figure S1. Growth curves of bacterial clones as measured by change in log-transformed ocular density (OD_{600}) over time (hours). Measures from the first 2.5 hours were excluded (blue line) as a rise in OD was observed independent of bacterial logistic growth which may skew the rolling regression process. Growth curves were independently replicated a total of 3 times (a - c) owing to cellular clumping which may have skewed OD measures. ("anc" = ancestral clones; "blank" = uninoculated wells; "control" = control clones; mix add" = clones from repeated phage treatment; "mix" = clones from treatment where phage were added once; "resist" = phage resistant clones; "susc" = susceptible clones; "sing_res" = in vitro clones resistant to one phage; "TP1" = *in vivo* clones from day 2; "TP2" = *in vivo* clones from day 4).

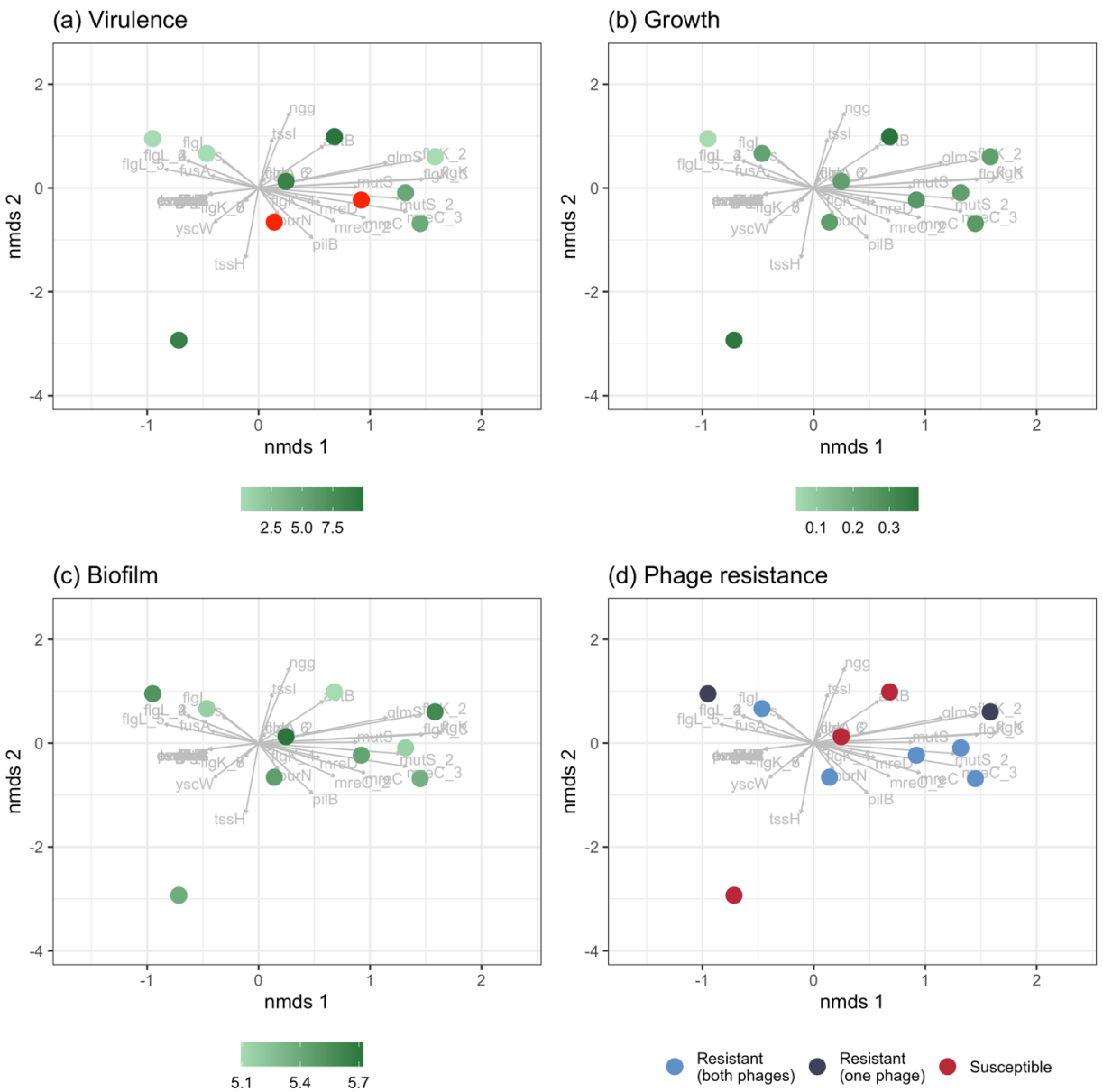

Figure S2. Associations between genetic similarity and phenotypic traits for *in vivo* clones. Individual points represent individual clones isolated at day 2 (n = 8) and day 4 (n = 2) of phage treatment. Genes that diverged in frequency *in vitro* from the ancestor are indicated in grey while *in vivo* clones are overlayed according to their individual genetic make-up. Across quantitative (a – c) and qualitative (d) phenotypic traits, no clustering in genotypes and clones of particular phenotypes is observed.

989 **Supplementary Tables**

990

991 Table S1. Susceptible colonies picked from *in vitro* phage treatments for phenotypic assays and

992 sequencing.

Phage resistance	Phage added	Treatment replicate	Clone number
Susceptible	Once	6	1
Susceptible	Once	6	2
Susceptible	Once	6	3
Susceptible	Once	3	4
Susceptible	Once	3	5
Susceptible	Once	3	6
Susceptible	Once	5	7
Susceptible	Once	5	8
Susceptible	Repeatedly	6	9
Susceptible	Repeatedly	6	10
Susceptible	Repeatedly	6	11
Susceptible	Repeatedly	1	12

993
994
995
996
997
998
999
1000
1001
1002
1003
1004
1005
1006
1007

1008 Table S2. Pairwise comparisons of resistance of *in vivo* clones from day 2 against phage from
1009 contemporary (day 2) and two future time-points (days 4 and 7). P-values adjusted using the Tukey
1010 method of comparing a family of three estimates. "SE" = standard error.

Contrast	Estimate	SE	z-ratio	p-value
Day 2 - Day 4	- 16.5	10	-1.65	0.2262
Day 2 - Day 7	- 16.5	10	-1.65	0.2264
Day 4 - Day 7	0.000001	5.32	0	1

1011
1012
1013
1014
1015
1016
1017
1018
1019
1020
1021
1022
1023
1024
1025
1026
1027
1028
1029
1030
1031

1032 Supplementary methods

1033 **Data cleaning of biofilm dataset.** In the *in vitro* dataset, one replicate in the control and one in
1034 the susceptible treatments were found to be outliers that significantly impacted data analysis. In
1035 the susceptible treatment, the outlier (711) had a value 2.9x greater than the group mean (246.9)
1036 and this was 2.7x greater than the next nearest value (266.1). Similarly, in the control group, the
1037 outlier (708.6) had a value 2.26x greater than the group mean (313.5) and this was 2.5x greater
1038 than the next nearest value (278). We subsequently determined the impact of these values
1039 individually and when together on model output by sequentially removing these from the dataset
1040 (Table S3, S4). Resistance was significant regardless of outlier removal (Table S3) as were
1041 comparisons between resistant and susceptible groups (Table S4). Although treatment became
1042 significant when the susceptible outlier was removed, all Tukey-HSD comparisons were non-
1043 significant. The only change detected in Tukey HSD comparisons was that between the single
1044 resistant and susceptible isolates which was found when the susceptible and both outliers were
1045 removed (Table S4).

1046

1047

1048

1049

1050

1051

1052

1053

1054 Table S3. The effect of outlier removal on the significance of model terms (treatment and phage
1055 resistance). Outlier removed states in which treatment each outlier was identified and subsequently
1056 removed. Significant p-values in bold.

1057

Model term	Outlier removed	Chi-sq value	P-value
Treatment * Resistance	None	1.32	0.5185
Treatment * Resistance	Susceptible	0.609	0.7824
Treatment * Resistance	Control	1.56	0.459
Treatment * Resistance	Both	0.785	0.675
Treatment	None	2.44	0.295
Treatment	Susceptible	6.207	**0.045**
Treatment	Control	1.501	0.472
Treatment	Both	4.53	0.104
Resistance	None	8.28	**0.016**
Resistance	Susceptible	15.44	**0.00044**
Resistance	Control	12.48	**0.0059**
Resistance	Both	19.13	**7.023e-05**

1058
1059

1060 Table S4. The effect of outlier removal on Tukey HSD contrasts comparing biofilm productivity

1061 between phage resistance groups. Significant p-values highlighted in bold.

Outlier removed	Contrast	Estimate	SE	t-ratio	p-value
None	Resistant – Single resistant	0.0916	0.210	0.436	0.901
None	Resistant – Susceptible	0.439	0.16	2.698	**0.0289**
None	Single resistant - Susceptible	0.348	0.2	1.74	0.207
Susceptible	Resistant – Single resistant	0.069	0.184	0.375	0.926
Susceptible	Resistant – Susceptible	0.597	0.165	3.618	**0.0029**
Susceptible	Single resistant - Susceptible	0.528	0.194	2.714	**0.0282**
Control	Resistant – Single resistant	0.087	0.193	0.449	0.8953
Control	Resistant – Susceptible	0.508	0.151	3.36	**0.0057**
Control	Single resistant - Susceptible	0.421	0.185	2.28	0.073
Both	Resistant – Single resistant	0.085	0.168	0.506	0.869
Both	Resistant – Susceptible	0.581	0.133	4.36	**0.0004**
Both	Single Resistant - Susceptible	0.496	0.162	3.067	**0.0119**

1062
1063
1064